JOURNAL
OF THE AMERICAN CHEMICAL SOCIETY

VOLUME 99, NUMBER 18 AUGUST 31, 1977

Carbon-13 Relaxation in Paramagnetic Complexes of Amino Acids. Structural and Dynamical Information on Nickel(II) Complexes of Histidine

Jens J. Led*[1a] and David M. Grant[1b]

Contribution from the Chemical Laboratory V, the H. C. Ørsted Institute, University of Copenhagen, 2100 Copenhagen, Denmark, and the Department of Chemistry, University of Utah, Salt Lake City, Utah 84112.
Received March 2, 1977

Abstract: The carbon-13 relaxation (T_1 and T_2) and the contact shift of histidine in water solution at pH 10.4, caused by the presence of Ni^{2+} ions in low concentration, have been studied over the temperature range from 293 to 388 K. The experimental data have been analyzed using generalized equations for the effect of any three-site exchange upon each of the three types of data. From this analysis it can be concluded that two Ni^{2+}-histidine complexes are present in an uneven ratio (1:0.08 at 298 K). The complexation reactions, carbon-13-electron hyperfine coupling constants, and the Ni^{2+}-carbon distances, also obtained from the data analysis, show that the structure of the abundant species corresponds closely to the structure of the octahedral bis(histidino)nickel(II) complex found in the crystal phase, while the rare species differ from this in that a carboxylate group has been disengaged from the Ni^{2+} ion. Activation parameters for the involved histidine exchange processes and the correlation time for the molecular diffusional rotation have been obtained. Furthermore, it is found that the electronic relaxation is consistent with the model of Bloembergen and Morgan, according to which it is caused by collision modulation of a transient zero-field splitting (ZFS) interaction. This interaction, the correlation time for its modulation, as well as the electron relaxation times, T_{1e} and T_{2e}, have been determined. From these results it is found that the spin-lattice relaxation of the carbon-13 nuclei caused by the unpaired electron is, with a single exception, dominated by the dipolar interaction, while the paramagnetic contribution to the carbon-13 spin-spin relaxation is influenced by the dipolar as well as the scalar interaction.

I. Introduction

In a previous work[2] we obtained both structural and dynamical parameters for a manganese(II) complex of histidine in water solution from the paramagnetic contact shift and the effect on the T_1 and T_2 relaxation times of the carbon-13 nuclei in the ligand caused by the unpaired electrons of the Mn^{2+} ions. In this investigation our attention is focused upon the corresponding complexation of histidine with nickel(II). For complexes of this ion the exchange rate of the ligands[3-9] as well as the spin relaxation times of the unpaired electrons[8-18] are in general very different from those of manganese(II) complexes,[2] and different dynamical regions of the contact shift and relaxation curves of the ligand carbons are therefore experimentally accessible and may be explored.

Thus, for nickel(II) complexes the metal-ligand exchange rates are several orders of magnitude slower[3-9] than in the case of manganese(II) complexes[2] and at room temperature are of comparable magnitude or smaller than the paramagnetic contact shift of the ligand carbon-13 nuclei. This feature permits one to study the onset of exchange with increasing temperature and to determine mechanistic details of metal-ligand exchange not to conveniently studied in fast exchanging metal complexes such as Mn^{2+} complexes, which at room temperature are already in the high temperature limit[2] as far as ligand exchange is concerned. Due to this inherent characteristic of Ni^{2+} complexes it has been possible in the present study to reveal the importance of at least two different nickel-histidine complexes in ligand exchange, and even though one of the complexes is significantly lower in concentration than the more abundant complex, its ligand exchange rate is more rapid, which permits data for this species easily to be sorted out from those of the dominant complex in the intermediate temperature region just above room temperature.

Generalized equations for the effect of any three-site exchange upon the T_1 and T_2 relaxation processes as well as the contact shift are developed as neither the Luz and Meiboom[7] and the Swift and Connick,[8] nor the Lam, Kuntz, and Kotowycz[19] specific formulations were adequate to treat the details of the nickel-histidine exchange mechanism. Using a matrix approach the extension to ligand exchange between four, five, or higher numbers of sites is readily apparent at least in principle from this work. As a practical matter, an exchange between more than three sites may pose a rather severe challenge experimentally, as criteria for proving uniqueness in the choice of mechanisms would be much more difficult to obtain as the number of interacting species increases.

In addition to ligand exchange rate parameters, one may also

obtain information on electron-nucleus hyperfine coupling constants, electron relaxation rates, interatomic distances, and overall reorientation rate parameters, as was obtained for the manganese(II)-histidine complex,[2] if one can determine the isotopic contact shift, $\Delta\omega_M$, and the mechanisms controlling the relaxation times, T_{1M} and T_{2M}, of the nuclei in the ligands, when these are in the metal-bound positions. In contrast with the manganese(II) case, where the electron spin relaxation rate is much slower than the overall molecular reorientation rate, the relaxation rate of the nickel(II) electrons is comparable in magnitude or faster than the reorientation rate.[8-18] This may change the relative importance of the dipolar and scalar contributions to the T_{1M} and T_{2M} relaxation times, making it more difficult to extract the above mentioned parameters from the experimental relaxation and contact shift data than in the case of a manganese(II) complex, where in general the T_{1M} relaxation of the carbon-13 nuclei are dominated totally by the dipolar interaction with the unpaired electrons, while the corresponding T_{2M} relaxation is completely controlled by the scalar interaction.[2] However, as shown in the present study, an unraveling of the relaxation mechanisms controlling T_{1M} and T_{2M} for the ^{13}C nuclei of nickel(II) complexes in water solution is possible, provided an extensive treatment is undertaken of paramagnetic shift and spin relaxation data over a large temperature range.

Thus, even though the dynamical parameters controlling the nuclear paramagnetic shifts and the spin relaxations of nickel(II) and manganese(II) complexes differ appreciably, we show that it is possible to obtain structural and dynamical information for the complexes of both metals.

II. Theoretical Considerations

The McConnell equations[20] for chemical exchange between three sites are given in matrix form as follows:

$$\dot{\mathbf{M}} = \mathbf{r}_1(\mathbf{M} - \mathbf{M}^0) + \mathbf{r}\mathbf{M} \tag{1}$$

$$\dot{\mathbf{G}} = (\omega + \mathbf{r}_2 + \mathbf{r})\mathbf{G} = \mathcal{S}\mathbf{G} \tag{2}$$

where the components (M_A, M_B, M_C, G_A, G_B, and G_C) of the **M** and **G** vectors are the z axis and x,y plane magnetizations, respectively, with $G_j = u_j + iv_j$, where u_j is the dispersion mode magnetization and v_j the absorption mode magnetization of the magnetic spin in the jth site. The various transition rate matrices associated with precession in a rotating frame moving with angular frequency ω, and with nuclear relaxation are given by:

$$\omega = \begin{vmatrix} -i(\omega_A - \omega) & 0 & 0 \\ 0 & -i(\omega_B - \omega) & 0 \\ 0 & 0 & -i(\omega_C - \omega) \end{vmatrix} \tag{3}$$

$$\mathbf{r}_k = \begin{vmatrix} -1/T_{kA} & 0 & 0 \\ 0 & -1/T_{kB} & 0 \\ 0 & 0 & -1/T_{kC} \end{vmatrix} \tag{4}$$

where $k = 1$ or 2 for respectively longitudinal or transverse relaxation. The chemical exchange rate matrix is:

$$\mathbf{r} = \begin{vmatrix} -1/\tau_A & 1/\tau_{BA} & 1/\tau_{CA} \\ 1/\tau_{AB} & -1/\tau_B & 1/\tau_{CB} \\ 1/\tau_{AC} & 1/\tau_{BC} & -1/\tau_C \end{vmatrix} \tag{5}$$

where $1/\tau_{ji}$ ($j \neq i$) is the rate by which ligands transfer from site j to i. The diagonal elements are given by $1/\tau_j = \Sigma_{i \neq j}(1/\tau_{ji})$. At magnetic equilibrium $\mathbf{M} = \mathbf{M}^0$ and $\dot{\mathbf{M}} = 0$. It is therefore evident from eq 1 that $\mathbf{r}\mathbf{M}^0 = 0$ allowing eq 1 to be written as:

$$\dot{\mathbf{M}} = (\mathbf{r}_1 + \mathbf{r})(\mathbf{M} - \mathbf{M}^0) = \mathcal{R}(\mathbf{M} - \mathbf{M}^0) \tag{6}$$

which is of a form similar to eq 2. $\mathcal{R}$ is all real while $\mathcal{S}$ contains imaginary quantities. Whenever the free ligand assigned to the label A is in considerable excess and $T_{kA}^{-1} \ll T_{kB}^{-1}, T_{kC}^{-1}$, which holds when B and C correspond to ligand sites in paramagnetic metal complexes as in the present study, the spin system will assume a steady-state condition where $\dot{M}_B = \dot{M}_C = \dot{G}_B = \dot{G}_C \cong 0$. Solving eq 6 and eq 2 using these conditions results in:

$$\frac{(M_B - M_B^0)}{(M_A - M_A^0)} = \frac{|\mathcal{R}^{ab}|}{|\mathcal{R}^{aa}|} \qquad \frac{(M_C - M_C^0)}{(M_A - M_A^0)} = \frac{|\mathcal{R}^{ac}|}{|\mathcal{R}^{aa}|} \tag{7}$$

$$G_B/G_A = |\mathcal{S}^{ab}|/|\mathcal{S}^{aa}| \qquad G_C/G_A = |\mathcal{S}^{ac}|/|\mathcal{S}^{aa}| \tag{8}$$

where $|\mathcal{R}^{aa}|$, $|\mathcal{R}^{ab}|$, and $|\mathcal{R}^{ac}|$ are the determinants of the cofactor matrices of the elements $\mathcal{R}_{aa}$, $\mathcal{R}_{ab}$, and $\mathcal{R}_{ac}$, respectively. A similar definition holds for the determinants of the corresponding $\mathcal{S}$ cofactor matrices. Thus on substitution of eq 7 and 8 into eq 6 and 2, respectively, we have:

$$\dot{M}_A = \left\{ \mathcal{R}_{aa} + \frac{\mathcal{R}_{ab}|\mathcal{R}^{ab}|}{|\mathcal{R}^{aa}|} + \frac{\mathcal{R}_{ac}|\mathcal{R}^{ac}|}{|\mathcal{R}^{aa}|} \right\} (M_A - M_A^0) = \frac{|\mathcal{R}|}{|\mathcal{R}^{aa}|}(M_A - M_A^0) \tag{9}$$

$$\dot{G}_A = \left\{ \mathcal{S}_{aa} + \frac{\mathcal{S}_{ab}|\mathcal{S}^{ab}|}{|\mathcal{S}^{aa}|} + \frac{\mathcal{S}_{ac}|\mathcal{S}^{ac}|}{|\mathcal{S}^{aa}|} \right\} G_A = \frac{|\mathcal{S}|}{|\mathcal{S}^{aa}|} G_A \tag{10}$$

Some confusion is avoided by noting that the labels in the chemical exchange matrix are transposed on the $1/\tau_{ij}$ in order to correspond with convention. Thus, $1/\tau_{AB} \equiv r_{ba} \equiv \mathcal{R}_{ba}$ and so forth for each of the other exchange terms. As $|\mathcal{S}^{aa}|$ is a complex number the imaginary quantities must be cleared from the denominator, before eq 10 can be used in computation.

Now as:

$$\dot{M}_A = -(1/T_{1,obsd})(M_A - M_A^0) \tag{11}$$

then

$$\frac{1}{T_{1,obsd}} = -\frac{|\mathcal{R}|}{|\mathcal{R}^{aa}|} = \frac{1}{T_{1A}} + \frac{1}{\tau_A} - \frac{\mathcal{R}_{ab}|\mathcal{R}^{ab}|}{|\mathcal{R}^{aa}|} - \frac{\mathcal{R}_{ac}|\mathcal{R}^{ac}|}{|\mathcal{R}^{aa}|} \tag{12}$$

Expanding the matrices yields for

$$\frac{1}{T_{1P}} = \frac{1}{T_{1,obsd}} - \frac{1}{T_{1A}} \tag{13}$$

the following:

$$\frac{f_A}{T_{1P}} = \frac{\frac{f_B}{\tau_{BA}T_{1B}}\left(\frac{1}{T_{1C}} + \frac{1}{\tau_{CA}} + \frac{1}{\tau_{CB}}\right) + \frac{f_C}{\tau_{CA}T_{1C}}\left(\frac{1}{T_{1B}} + \frac{1}{\tau_{BA}} + \frac{1}{\tau_{BC}}\right) + \frac{f_B}{\tau_{BA}\tau_{BC}T_{1C}} + \frac{f_C}{\tau_{CA}\tau_{CB}T_{1B}}}{\left(\frac{1}{T_{1B}} + \frac{1}{\tau_{BA}} + \frac{1}{\tau_{BC}}\right)\left(\frac{1}{T_{1C}} + \frac{1}{\tau_{CA}} + \frac{1}{\tau_{CB}}\right) - \frac{1}{\tau_{BC}\tau_{CB}}} \tag{14}$$

where the partial molar quantities f_A, f_B, and f_C are given by:

$$\frac{f_B}{f_A} = \frac{M_B^0}{M_A^0} = \frac{\tau_{BA}}{\tau_{AB}} = \frac{q_B[B]}{[A]}$$
$$\frac{f_C}{f_A} = \frac{M_C^0}{M_A^0} = \frac{\tau_{CA}}{\tau_{AC}} = \frac{q_C[C]}{[A]} \quad (15)$$
$$\frac{f_C}{f_B} = \frac{M_C^0}{M_B^0} = \frac{\tau_{CB}}{\tau_{BC}} = \frac{q_C[C]}{q_B[B]}$$

where q_B and q_C are the numbers of ligands in complex B and C, respectively. For a three-site exchange with no direct exchange between the two paramagnetic sites B and C, that is, $\tau_{BC}^{-1} = \tau_{CB}^{-1} = 0$, eq 14 reduces to:

$$\frac{f_A}{T_{1P}} = \frac{f_B}{(T_{1B} + \tau_{BA})} + \frac{f_C}{(T_{1C} + \tau_{CA})} \quad (16)$$

showing that the Luz and Meiboom relationship[7] also holds under these conditions. Similarly, if species A and C do not directly exchange (i.e., $\tau_{CA}^{-1} = 0$) one obtains an expression which is simpler than eq 14:

$$\frac{f_A}{T_{1P}} = \frac{f_B(T_{1C} + \tau_{CB}) + f_C T_{1B}}{(T_{1B} + \tau_{BA})(T_{1C} + \tau_{CA}) + (f_C \tau_{BA} T_{1B}/f_B)} \quad (17)$$

One may proceed to obtain expressions for the contact shift, $\Delta\omega_P = \omega_{obsd} - \omega_A$, and for $T_{2P}^{-1} = T_{2,obsd}^{-1} - T_{2A}^{-1}$ from eq 10 by recognizing that the imaginary part of G_A will vanish if ω is selected to be ω_{obsd}, the center of the ligand absorption line under the influence of exchange with the paramagnetic metal. Furthermore, the real part of G_A will decay with a characteristic time $T_{2,obsd}$. Therefore:

$$\frac{1}{T_{2,obsd}} = -\mathrm{Re}\left\{\frac{|\mathcal{S}|}{|\mathcal{S}^{aa}|}\right\} = \frac{1}{T_{2A}} + \frac{1}{\tau_A} - \mathrm{Re}\left\{\frac{|\mathcal{S}^{ab}|}{|\mathcal{S}^{aa}|} + \frac{|\mathcal{S}^{ac}|}{|\mathcal{S}^{aa}|}\right\} \quad (18)$$

$$0 = \mathrm{Im}\left\{\frac{|\mathcal{S}|}{|\mathcal{S}^{aa}|}\right\} = -(\omega_A - \omega_{obsd}) + \mathrm{Im}\left\{\frac{|\mathcal{S}^{ab}|}{|\mathcal{S}^{aa}|} + \frac{|\mathcal{S}^{ab}|}{|\mathcal{S}^{aa}|}\right\} \quad (19)$$

Thus, solution of eq 19 for $\Delta\omega_P$ yields a value for ω which can then be used in eq 18 to calculate T_{2P}^{-1}. Expanding eq 18 and 19 and eliminating imaginary terms in the denominators of these two expressions yields the following equations:

$$\frac{1}{T_{2P}} = \frac{1}{T_{2,obsd}} - \frac{1}{T_{2A}} = \frac{FD + GE}{D^2 + E^2} \quad (20)$$

and

$$\Delta\omega_P = (\omega_{obsd} - \omega_A) = \frac{GD - FE}{D^2 + E^2} \quad (21)$$

where:

$$D = \left(\frac{1}{T_{2B}} + \frac{1}{\tau_{BA}} + \frac{1}{\tau_{BC}}\right)\left(\frac{1}{T_{2C}} + \frac{1}{\tau_{CA}} + \frac{1}{\tau_{CB}}\right) - \frac{1}{\tau_{BC}\tau_{CB}} - \Delta\omega_B\Delta\omega_C \quad (22)$$

$$E = \Delta\omega_B\left(\frac{1}{T_{2C}} + \frac{1}{\tau_{CA}} + \frac{1}{\tau_{CB}}\right) + \Delta\omega_C\left(\frac{1}{T_{2B}} + \frac{1}{\tau_{BA}} + \frac{1}{\tau_{BC}}\right) \quad (23)$$

$$F = \frac{f_B}{f_A\tau_{BA}}\left[\frac{1}{T_{2B}}\left(\frac{1}{T_{2C}} + \frac{1}{\tau_{CA}} + \frac{1}{\tau_{CB}}\right) + \frac{1}{T_{2C}\tau_{BC}} - \Delta\omega_B\Delta\omega_C\right] + \frac{f_C}{f_A\tau_{CA}} \times\left[\frac{1}{T_{2C}}\left(\frac{1}{T_{2B}} + \frac{1}{\tau_{BA}} + \frac{1}{\tau_{BC}}\right) + \frac{1}{T_{2B}\tau_{CB}} - \Delta\omega_B\Delta\omega_C\right] \quad (24)$$

$$G = \frac{f_B}{f_A\tau_{BA}}\left[\Delta\omega_B\left(\frac{1}{T_{2C}} + \frac{1}{\tau_{CA}} + \frac{1}{\tau_{CB}}\right) + \Delta\omega_C\left(\frac{1}{T_{2B}} + \frac{1}{\tau_{BC}}\right)\right] + \frac{f_C}{f_A\tau_{CA}}\left[\Delta\omega_B\left(\frac{1}{T_{2C}} + \frac{1}{\tau_{CB}}\right) + \Delta\omega_C\left(\frac{1}{T_{2B}} + \frac{1}{\tau_{BA}} + \frac{1}{\tau_{BC}}\right)\right] \quad (25)$$

If $\tau_{BC}^{-1} = \tau_{CB}^{-1} = 0$ then eq 20 and 21 give the Swift and Connick expressions[8] for T_{2P}^{-1} and $\Delta\omega_P^{-1}$. In eq 22-25 $\Delta\omega_B = \omega_B - \omega_{obsd}$ and $\Delta\omega_C = \omega_C - \omega_{obsd}$. Should it be more convenient to work in terms of $\Delta\omega_P$, then:

$$\Delta\omega_B = (\omega_B - \omega_A) - \Delta\omega_P$$
$$\Delta\omega_C = (\omega_C - \omega_A) - \Delta\omega_P \quad (26)$$

In many cases the free ligand will be in considerable excess and therefore $f_A \cong 1$. Furthermore, if all metal ions are complexed in one form or another we have the additional relationship:

$$\frac{f_B}{q_B} + \frac{f_C}{q_C} = f_M \quad (27)$$

where $f_M = [M_0]/[L_0]$ and $[M_0]$ and $[L_0]$ are the total concentrations of metal and ligand, respectively.

The relaxation rates, T_{kj}^{-1}, in the metal-bound positions (j = B, C) can be expressed by the modified Solomon-Bloembergen equations:[21-23]

$$\frac{1}{T_{1j}} = \frac{2}{15}\frac{S(S+1)g^2\beta^2\gamma_I^2}{r_j^6}\left[\frac{3\tau_{c,1}}{1 + \omega_I^2\tau_{c,1}^2} + \frac{7\tau_{c,2}}{1 + \omega_S^2\tau_{c,2}^2}\right] + \frac{2}{3}S(S+1)\left(\frac{A}{\hbar}\right)^2\left[\frac{\tau_{e,2}}{1 + \omega_S^2\tau_{e,2}^2}\right] \quad (28)$$

$$\frac{1}{T_{2j}} = \frac{1}{15}\frac{S(S+1)g^2\beta^2\gamma_I^2}{r_j^6} \times\left[4\tau_{c,1} + \frac{3\tau_{c,1}}{1 + \omega_I^2\tau_{c,1}^2} + \frac{13\tau_{c,2}}{1 + \omega_S^2\tau_{c,2}^2}\right] + \frac{1}{3}S(S+1)\left(\frac{A}{\hbar}\right)^2\left[\tau_{e,1} + \frac{\tau_{e,2}}{1 + \omega_S^2\tau_{e,2}^2}\right] \quad (29)$$

where the correlation times $\tau_{c,1}$, $\tau_{c,2}$, $\tau_{e,1}$, and $\tau_{e,2}$ are:

$$\frac{1}{\tau_{c,k}} = \frac{1}{\tau_R} + \frac{1}{T_{ke}} + \frac{1}{\tau_j} \quad (30)$$

$$\frac{1}{\tau_{e,k}} = \frac{1}{T_{ke}} + \frac{1}{\tau_j} \quad (31)$$

Here τ_R^{-1} is the rotational reorientation rate, and T_{ke}^{-1} is the longitudinal or transversal relaxation rate for k = 1 or 2, respectively, while τ_j^{-1} is the reciprocal lifetimes of the nucleus in the j site (j = B, C), identical with the diagonal B or C elements of **r**. The individual exchange rates, τ_{ji}^{-1} ($j \neq i$) are given by the Eyring equation:

$$\frac{1}{\tau_{ji}} = \frac{kT}{h}\exp\left(-\frac{\Delta H_{ji}^{\ddagger}}{RT} + \frac{\Delta S_{ji}^{\ddagger}}{R}\right) \quad (32)$$

while the Arrhenius equation:

$$\tau_R = \tau_R^0 \exp(E_R/RT) \quad (33)$$

is used to characterize the temperature dependence of the reorientational motion. Finally, as an ion with an electron triplet group state, Ni^{2+} has only one T_{1e} relaxation time and one T_{2e} relaxation time given by:[11,24,25]

$$\frac{1}{T_{1e}} = \frac{\Delta^2}{25}[4S(S+1) - 3]\left[\frac{\tau_v}{1 + \omega_S^2\tau_v^2} + \frac{4\tau_v}{1 + 4\omega_S^2\tau_v^2}\right] \quad (34)$$

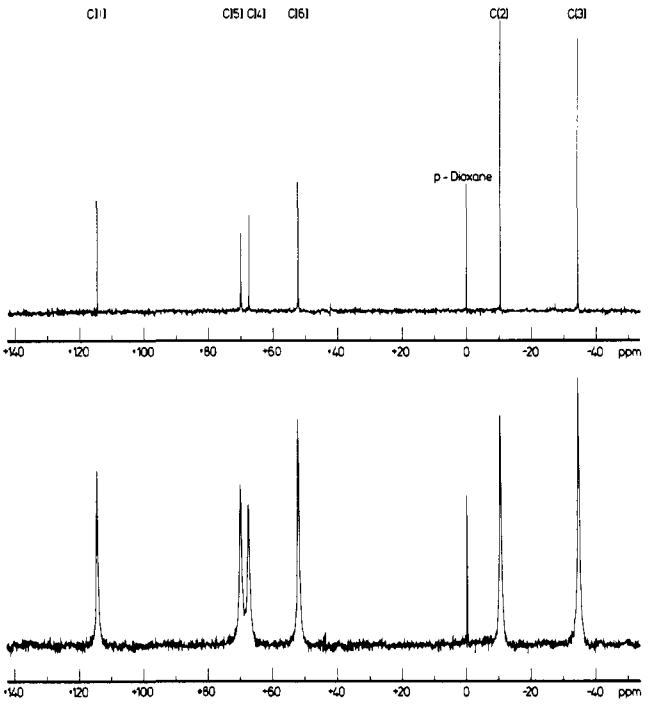

Figure 1. Carbon-13 spectra at 23.5 kG of 1.90 M solutions of histidine in water at pH 10.4 and 343 K, with *p*-dioxane as internal standard. The solution corresponding to the lower spectrum contains, in addition, 1.00×10^{-2} M $NiCl_2$.

$$\frac{1}{T_{2e}} = \frac{\Delta^2}{50}[4S(S+1) - 3] \times \left[3\tau_v + \frac{5\tau_v}{1+\omega_S^2\tau_v^2} + \frac{2\tau_v}{1+4\omega_S^2\tau_v^2}\right] \quad (35)$$

where τ_v is a time characteristic for the random field modulation, which causes the electronic relaxation, while Δ, the zero-field splitting parameter (ZFS), measures the strength of the interacting field. The condition for the rigorous application of the two formulas is:[26]

$$\tau_v \ll T_{1e}, T_{2e} \quad (36)$$

The form of eq 34 and 35 holds regardless of the mechanism that gives rise to the relaxation, while τ_v as well as Δ depend upon the physical origin of the relaxation. Again an Arrhenius expression is used to give the temperature dependence of τ_v:

$$\tau_v = \tau_v^0 \exp(E_v/RT) \quad (37)$$

Finally, assuming a Curie law temperature dependence and an effective isotopic g tensor, the contact shift, $\Delta\omega_{M,j} = \omega_j - \omega_A$ (j = B, C), between the ligand nuclei in the unbound and metal-bound positions is given by:

$$\frac{\Delta\omega_{M,j}}{\omega_I} = \frac{\Delta H}{H} = \frac{g\beta S(S+1)}{3\hbar\gamma_N kT} A_j \quad (38)$$

In the following calculations $\Delta\omega_{M,j}$ was approximated by $\Delta\omega_j$, neglecting $\Delta\omega_P$ in eq 26. This approximation is reasonable for small values of the ratios f_B/f_A and f_C/f_A (eq 15).

III. Experimental Section

Highly purified L-histidine (free base) and analytical reagent $NiCl_2 \cdot 6H_2O$ were used. The nickel salt was dried in vacuo at 220 °C until the water of crystallization was expelled. All samples were 1.90 M solutions of histidine in distilled, deionized water at pH 10.4 and with a concentration of Ni^{2+} ranging from 0 to 0.2 M. All concentrations were determined by weighing and volumetric measurements. The preparations were carried out in a nitrogen atmosphere using water which had been purged with nitrogen for 30 min and the samples were sealed off in vacuo. Prepared in this manner no precipitation of $Ni(OH)_2$ occurred and the samples as well as their spectra remained unchanged during the period of the study.

Table I. Preexponential Factors, A, and Activation Energies, E_R, Corresponding to $(T_1^0)^{-1}$ for the Histidine Carbons Including 1σ Confidence Limits

	$A \times 10^5$, s^{-1}	E_R, kcal mol^{-1}
C(1)	0.56 ± 0.15	6.06 ± 0.16
C(2)	10.1 ± 2.3	5.76 ± 0.14
C(3)	11.9 ± 3.1	6.01 ± 0.17
C(4)	1.0 ± 0.3	5.85 ± 0.77
C(5)	5.3 ± 1.1	6.19 ± 0.15
C(6)	4.6 ± 0.7	6.22 ± 0.11

Natural abundance, ^1H noise-decoupled ^{13}C NMR spectra were obtained in the Fourier transform mode at 25.2 MHz using a Varian XL100-15 spectrometer. Typical ^{13}C spectra of the histidine samples are shown in Figure 1. The 90° pulse of the probe (V4415) used for the line width and contact shift measurements were 100 μs for a carrier frequency which differs 500 Hz from the resonance line, while in the T_1 experiment (probe V4412) the 90° pulse was 16 μs, practically independent of the distance from the carrier frequency within the frequency range of the spectrum. The 100 MHz rf field for ^1H noise decoupling was produced by a Hewlett-Packard 5105A frequency synthesizer combined with a Hewlett-Packard 5110B frequency synthesizer driver and amplified with a 10W ENI Model 310L wide-band rf amplifier connected with a 100-MHz filter. A decoupling field intensity of 9 W with negligible reflection was used in all experiments. The samples were contained in 10-mm NMR tubes, while the deuterium resonance of D_2O or dimethyl-d_6 sulfoxide placed in the annulus between the 10-mm tube and a 12-mm NMR tube was used as a lock signal. The temperature control was accomplished by means of the Varian temperature control unit using an air flow of 35 std ft^3/h. The samples were allowed to temperature equilibrate in the probe for at least 20 min before the experiments were started. The thermometer used for the temperature measurements was immersed in a 1.90 M histidine solution identical with the sample stock solution placed in a 12-mm NMR tube, the end of the thermometer being 25 mm above the bottom of the tube. The power level of the rf decoupling field as well as the air flow was identical with those used in the experiments. When measured this way before and after an experiment the temperature was reproducible within ±0.5 °C. The use of a histidine solution in the temperature measurements eliminates an error that otherwise would have been introduced by an extra heating of the histidine solution of 2-4 °C not observed when the thermometer was immersed in pure water or an organic solvent. This heating effect did not occur in the absence of the ^1H noise-decoupling field and was attributed to dielectric losses in the electrolytic solution.

T_1 relaxation times were evaluated from ^1H-decoupled, partially relaxed Fourier transform spectra obtained using the 90°-T-180°-τ-90°-T pulse sequence,[29] where in all experiments $T \geq 4T_1$. Each T_1 value was extracted from 12-15 spectra. For nonparamagnetic samples 50-100 FID signals were accumulated per spectrum, while in the case of the paramagnetic samples each spectrum was obtained from 500 to 1000 FID signals. An exponential multiplication of the FID signals corresponding to an increased line width of 3-5 Hz was employed. Additionally, by using an interactive disk system all the compounded FID signals corresponding to the 12-15 partially relaxed spectra were accumulated over the same period of time, thereby minimizing errors caused by fluctuation of experimental parameters during the experiment, such as homogeneity drift and temperature fluctuations. This was accomplished by accumulating series of FID signals where each series contains one FID signal corresponding to each of the 12-15 different τ values. The FID signals were stored in separate areas corresponding to the individual τ values directly on the disk, which unlike the computer memory can contain all 12-15 different FID signals simultaneously. Since all the measured T_1 values that contribute significantly to the calculated T_{1P} values (150 ms $< T_{1P} <$ 800 ms) are relatively short, any error due to diffusion in the sample is considered negligible.[30] Due to the short 90° pulse of the probe the T_1 values for all six carbons could be obtained from the same set of partially relaxed spectra. The T_1 values were

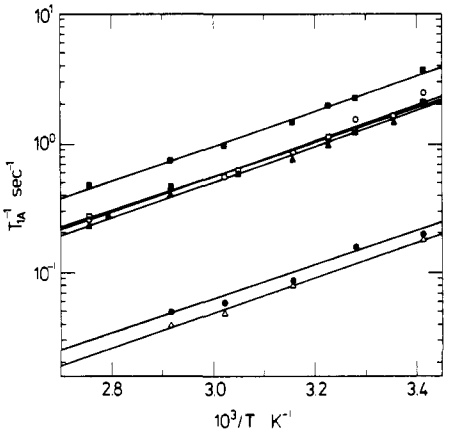

Figure 2. Temperature variation of the experimental ^{13}C spin-lattice relaxation rates, T_{1A}^{-1} (= $(T_1^0)^{-1}$), for the histidine carbons, obtained at 23.5 kG from a 1.90 M solution of histidine in water at pH 10.4: △ C(1); □ C(2); ■ C(3); ● C(4); ○ C(5); ▲ C(6). The curves were computed using the activation parameters in Table I, corresponding to the best fit.

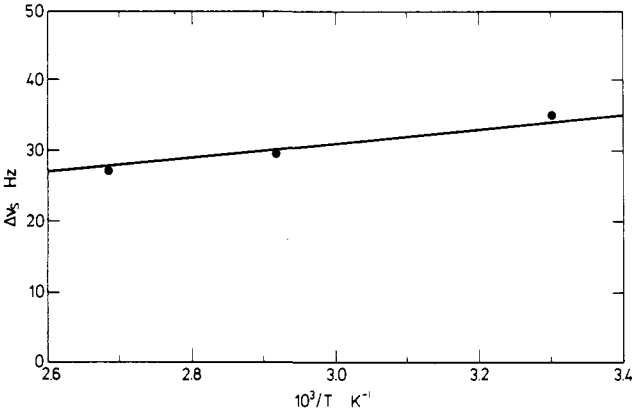

Figure 3. Temperature variation of the paramagnetic susceptibility shift of the ^{13}C signal of *p*-dioxane, for $[Ni^{2+}]$ = 0.174 M and a magnetic field of 23.5 kG. The shift was measured as described in ref 2.

extracted from these spectra by a least-squares fit of the exponential equation

$$y = S(\infty) - S(t) = 2S(\infty)\exp(-\tau/T_1) \qquad (39)$$

directly to the experimental line intensities in order to assure an equal weighting of the data points. The 1σ standard deviation of the obtained T_1 values were 2-5% except for the longer T_1 values of the quaternary ^{13}C in the nonparamagnetic sample where the standard deviations were up to 12%. For this sample the T_1 values (T_1^0) were determined at fewer temperatures than for the paramagnetic samples. In order to obtain the T_{1P} values corresponding to the $T_{1,obsd}$ data at the intermediate temperatures, the necessary T_{1A} values (= T_1^0 by neglecting paramagnetic contribution to the relaxation of the ^{13}C nuclei outside the first coordination sphere[2]) were calculated from eq 33 by using activation energies and preexponential factors obtained from least-squares fit of eq 33 to the experimental $1/T_1^0$ data. These parameters are given in Table I, while the fit is shown in Figure 2.

The experimental transverse relaxation times were measured from the line width at half height assuming a Lorentzian line shape and the relation $\Delta\nu_{1/2} = 1/(\pi T_2)$. A delay of $4T_1$ was applied between 90° pulses to assure the validity of this equation.[31] To minimize errors due to differences in temperature and inhomogeneity broadening, corresponding values of $T_{2,obsd}$ and T_{2A} (= T_2^0) were measured sequentially as pairs. FID signals (200-300) were accumulated for each spectrum of the nonparamagnetic samples, while 5000-70 000 FID signals were stored for each spectrum of the paramagnetic samples, the exact numbers depending on the paramagnetic concentration and the temperature. In all T_2 experiments the sweep width was 5000 Hz, while 4096 data points were used to define the absorption mode

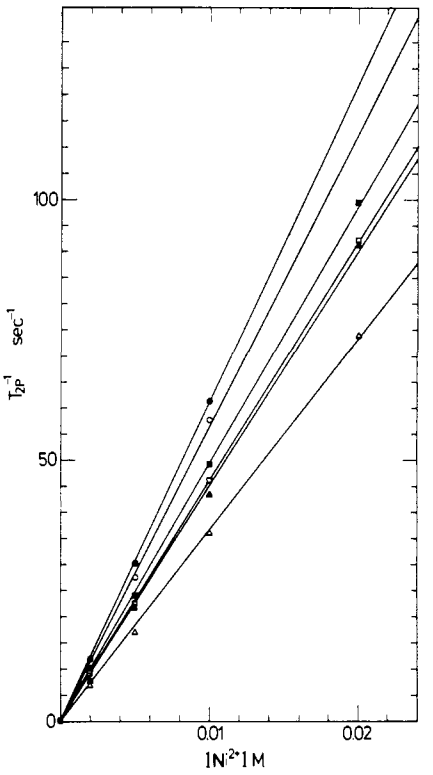

Figure 4. Experimental T_{2P}^{-1} relaxation rates for histidine carbons as function of $[Ni^{2+}]$, obtained at 23.5 kG from a 1.90 M solution of histidine in water at pH 10.4 and for $[Ni^{2+}]$ in the range 2.00×10^{-3}-2.00×10^{-2} M: △ C(1); □ C(2); ■ C(3); ● C(4); ○ C(5); ▲ C(6).

spectrum. The accuracy of the line widths, obtained from expanded spectra of the individual lines as well as the chemical shifts measured relative to the ^{13}C signal of the internal dioxane reference, were estimated to be $\lesssim \pm 0.5$ Hz.

The static magnetic susceptibility was measured using the NMR method of Evans[32] and Deutsch and Poling[33] as described earlier.[2] The samples were identical with those used in the ^{13}C relaxation and contact shift experiments, except for a higher concentration of paramagnetic ions in the paramagnetic sample.

IV. Results and Discussion

A. The Effective Electron Magnetic Moment. The magnetic moment of the unpaired electrons of the Ni^{2+} ion was obtained from the paramagnetic susceptibility shift of the ^{13}C line from the internal *p*-dioxane reference, assuming a Curie's law temperature dependence. A least-squares fit to the experimental shift data shown in Figure 3 gave an electronic magnetic moment of 3.02 ± 0.05 μ_B, in good agreement with a magnetic moment of 3.16 μ_B found for the unpaired electrons in the octahedral $Ni(His)_2$-H_2O complex (His = histidine) in the solid phase[34] as well as with the range of 2.9-3.2 μ_B within which the electronic magnetic moments of other crystalline, octahedral nickel(II) complexes have been found.[35] The result obtained here, which corresponds to an effective *g* value of 2.13 ± 0.04, indicates therefore that no nickel(II) complex with symmetry lower than octahedral is formed in ample abundance in the aqueous solution of histidine and Ni^{2+} ions, used in the present study. This indication is fully supported by the results discussed below.

B. Qualitative Evaluation of Relaxation and Contact Shift Data. $1/T_{1P}$, $1/T_{2P}$, and $\Delta\omega_P$ data were obtained in the temperature region from 293 to 388 K. Due to drastic changes in all three types of data over this temperature range, several different concentrations of Ni^{2+} ions had to be employed in order to assure a sufficient accuracy of measurement over the entire region. At several temperatures data corresponding to more than one concentration of the Ni^{2+} ions were obtained

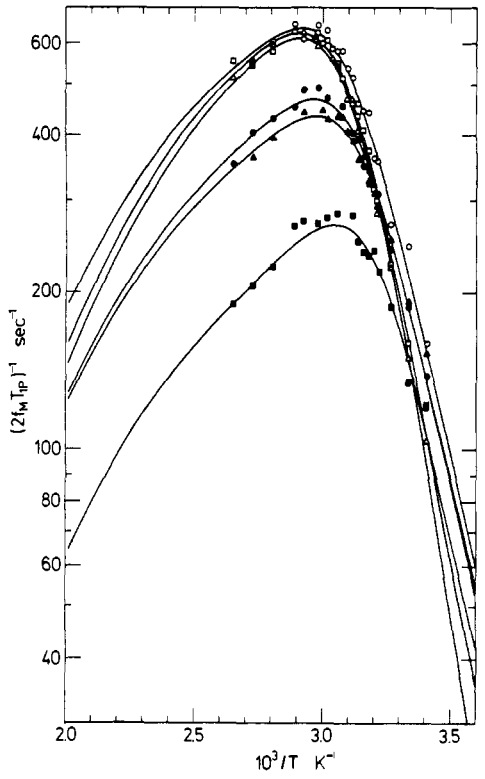

Figure 5. Temperature variation of the normalized experimental T_{1P}^{-1} relaxation rates for the histidine carbons, obtained at 23.5 kG from a 1.90 M solution of histidine in water at pH 10.4 and with $[Ni^{2+}] = 2.00 \times 10^{-3}$–$2.00 \times 10^{-2}$ M: △ C(1); □ C(2); ■ C(3); ● C(4); ○ C(5); ▲ C(6). The curves were computed using $\delta\Delta H = 2.5$ kcal mol^{-1}, $\delta\Delta S = -4.3$ cal mol^{-1} deg^{-1}, and the parameters in Tables III-V, corresponding to the best fit.

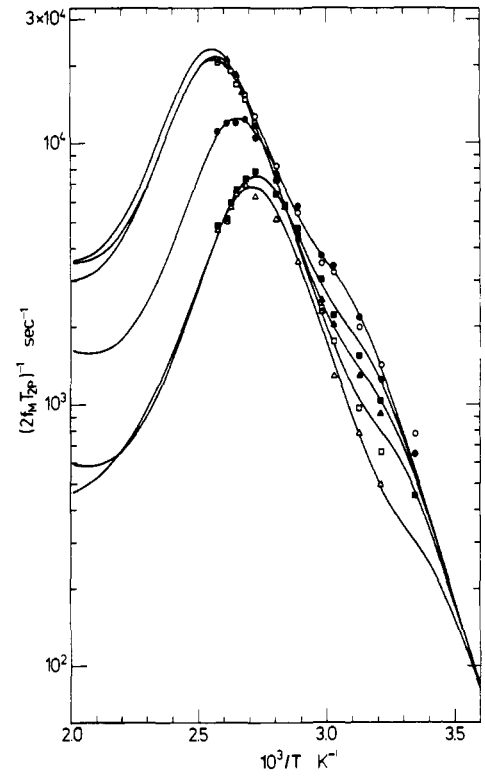

Figure 6. Temperature variation of the normalized experimental T_{2P}^{-1} relaxation rates for the histidine carbons, obtained at 23.5 kG from a 1.90 M solution of histidine in water at pH 10.4 and with $[Ni^{2+}] = 1.00 \times 10^{-3}$–$2.00 \times 10^{-2}$ M: △ C(1); □ C(2); ■ C(3); ● C(4); ○ C(5); ▲ C(6). The curves were computed using $\delta\Delta H = 2.5$ kcal mol^{-1}, $\delta\Delta S = -4.3$ cal mol^{-1} deg^{-1} and the parameters in Tables III-V, corresponding to the best fit.

to check the compatibility of the samples. The linear concentration dependence for the $1/T_{2P}$ that appears from Figure 4 not only demonstrates this compatibility, but shows also that the nature of the complexation taking place in the solutions is independent of the concentration of the Ni^{2+} ions within the concentration range used here.

The experimental data thus obtained are shown in Figures 5-7 for all six histidine carbons, normalized to $[Ni^{2+}] = 0.010$ M. In all cases where data for more than one concentration of the Ni^{2+} ions were obtained, a weighted average was used. The most conspicuous feature of the data plots is their considerable curvature. In general, this provides a rich source of information. More specifically, the values of all three types of data for each individual carbon increase with increasing temperature in the lower part of the experimental temperature region. According to the simple two-site exchange model as described by Swift and Connick[8] and Luz and Meiboom[7] this shows, unambiguously, that the slow exchange limit applies, i.e., the exchange rate of the ligands between the unbound and metal-bound positions are smaller than the difference between chemical shifts of the two positions between which the exchange occur. This should be compared with the results obtained on the basis of the same model for the corresponding Mn^{2+} complex,[2] where the fast exchange limit was found to apply; i.e., the exchange rate of the ligands is larger than the corresponding difference in chemical shift. This difference in exchange rate is in close agreement with the findings of other authors[3-9] and reflects the difference in stability of the Ni^{2+} and Mn^{2+} complexes.[36-40] Furthermore, the insignificant magnitudes at the lowest experimental temperatures of all three types of data, and, in particular, of the relaxation rates, demonstrate the absence of any appreciable contribution from outer sphere interaction and justify therefore the approximation $T_{1A} = T_1^0$. Since the time scale for such an interaction is expected to be of the same order of magnitude as the time scale for the molecular diffusions, even a relatively small effect of this type could influence the data in this region of the experimental temperature range.

A more detailed inspection of the data plots reveals, however, some most remarkable features of the data. Thus, from Figure 6 as well as Figure 4 it is apparent that a dispersion of the $1/T_{2P}$ data for different ^{13}C nuclei appears in the temperature region where $1/T_{2P}$, according to Figure 6, *increases* with increasing temperature. Obviously, this characteristic is incompatible with the model for a simple two-site exchange process,[8] where the ligands exchange between one paramagnetic site and their unbound position. According to this model all $1/T_{2P}$ relaxation rates should be totally controlled by the common exchange rate, and thereby identical.[41] Conversely, according to the same model a dispersion of the $1/T_{2P}$ values for the different carbons is only compatible with the fast exchange condition.[41] Therefore, the dispersion of the $1/T_{2P}$ data in the lower part of the experimental temperature region reveals that the obtained data cannot be completely interpreted on the basis of the simple two-site exchange model and a more complex exchange scheme must apply in the present case; i.e., more than one type of complex between Ni^{2+} and histidine must be present. This disclosure is further supported by the observed paramagnetic shift of the C(1) carbon atom, which at low temperature has small and *negative* values, but at about 340 K passes through zero and assumes increasingly *positive* values above this temperature. Also this feature is in conflict with a simple two-site exchange process, since it would imply a concomitant change in sign of the C(1)-electron hyperfine coupling constant A[C(1)]. On the other hand, this feature is immediately intelligible if the C(1) carbon can exist in at least

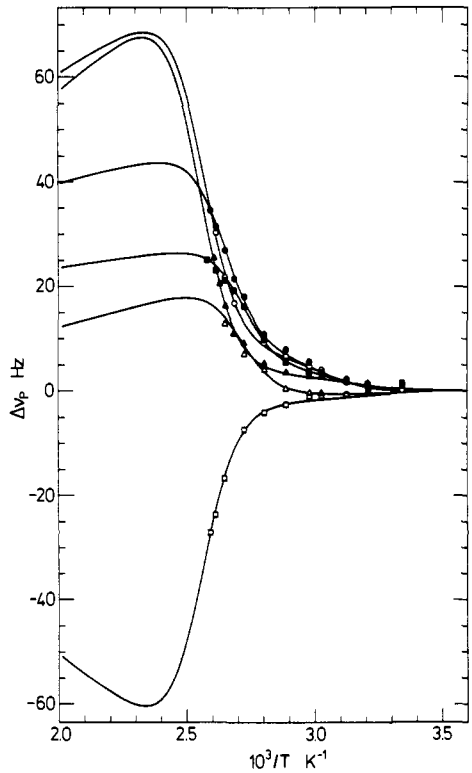

Figure 7. Temperature variation of the experimental contact shift, $\Delta\nu_P$, of the histidine carbons obtained at 23.5 kG from a 1.90 M solution of histidine in water at pH 10.4 and with $[Ni^{2+}] = 5.00 \times 10^{-3}$–$2.00 \times 10^{-2}$ M. Positive shifts are toward lower field and negative shifts toward higher field: △ C(1); □ C(2); ■ C(3); ● C(4); ○ C(5); ▲ C(6). The curves were computed using $\delta\Delta H = 2.5$ kcal mol^{-1}, $\delta\Delta S = -4.3$ cal mol^{-1} deg^{-1} and the parameters in Tables III-V, corresponding to the best fit.

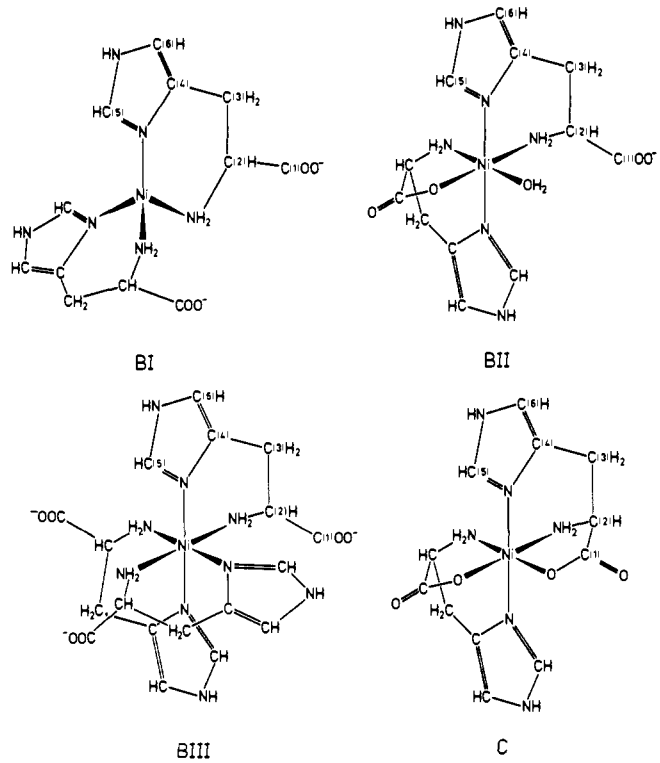

Figure 8. Schematic structures of possible histidine-Ni^{2+} complexes, see text.

two paramagnetic sites for which $A[C(1)]$ has opposite signs. In addition to these two characteristics directly apparent from a qualitative inspection, it was found impossible to fit the simple two-site model to the data set corresponding to any of the individual ligand carbons. This also includes attempts to take into account pseudocontact shift both with a T^{-1} temperature dependence[42-45] and a T^{-2} temperature dependence.[46,47] The failure of this model is already indicated by the small effective g value.

From the results of this evaluation it must, therefore, be concluded that the simple two-site exchange process is insufficient to account for the experimental data owing to the presence of more than one type of Ni^{2+}-histidine complex and, consequently, a more complex reaction scheme. Therefore, the general three-site model described in section II must be brought into play.

C. Models of Three-Site Chemical Exchange for the Nickel(II)–Histidine Interaction. The general scheme for exchange between three sites is shown in eq 40, where, as in section II, A is the free ligands while B and C are assigned to the two types of paramagnetic sites. In order to account for the experimental

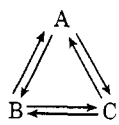

(40)

data at least two of the three possible exchange processes must be active. This leaves us with a total of three exchange models, i.e., the three-way exchange in eq 40, a model where exchange occurs between A and both B and C, but without exchange between the two paramagnetic sites:

$$B \rightleftarrows A \rightleftarrows C \qquad (41)$$

and a scheme where exchange takes place between A and one of the two paramagnetic sites, as well as between these two mutually:

$$A \rightleftarrows B \rightleftarrows C \qquad (42)$$

Before attempts are made to fit these models to the experimental data, it is helpful to examine what possible candidates there are for the two metal complexes and by means of these to express eq 40-42 in a more tangible form. Here an octahedral $Ni(His)_2$ complex, similar to that found in the crystal phase,[48] is by far the most likely complex.[37-40] This species, to which C is arbitrarily assigned, is shown in Figure 8 together with other possible candidates. Among these is a tetrahedral complex, BI, similar to the tetrahedral $Co(His)_2$ complex suggested by McDonald and Phillips.[49] Also a complex of the type BII, where one of the carboxylate groups has been replaced as a chelating group by a water molecule, is a potential candidate, since the dissociation of Ni^{2+}-amino acid complexes most likely starts with a detachment of the labile carboxylate group.[6] Finally, it has been suggested[39] that an octahedral complex of the type $Ni(His)_3$, shown as BIII in Figure 8, should occur in water solution containing a large surplus of histidine relative to the Ni^{2+} ion concentration, as in the present study.

More specific complexation reactions corresponding to the three models in eq 40-42 can now be proposed. Examples where one of the paramagnetic sites is assigned to complex C, while the second type is attributed to one of the three suggested B complexes are given below. M stands for the Ni^{2+} ion, while L is the histidine ligand. Thus for B ≡ BI one has:

$$\underset{(C)}{ML_2} + \underset{(A)}{L'} \underset{k_{-1}}{\overset{k_1}{\rightleftarrows}} \underset{(C)}{MLL'} + \underset{(A)}{L} \qquad (43)$$

$$\underset{(BI)}{ML_2} + \underset{(A)}{L'} \underset{k_{-2}}{\overset{k_2}{\rightleftarrows}} \underset{(BI)}{MLL'} + \underset{(A)}{L} \qquad (44)$$

$$\underset{(C)}{ML_2} \underset{k_{-3}}{\overset{k_3}{\rightleftarrows}} \underset{(BI)}{ML_2} \qquad (45)$$

where L and L′ are used to distinguish individual histidine molecules. Since $[L_0] \gg [M_0]$, where $[L_0]$ and $[M_0]$ are the initial concentrations of the ligands and the metal ions, respectively, these reactions are of pseudo first order and the exchange rates are therefore:

$$\frac{1}{\tau_{CA}} = \frac{k_1[L_0]}{2}; \frac{1}{\tau_{AC}} = \frac{f_C}{f_A}\frac{1}{\tau_{CA}} = \frac{f_C}{f_A}\frac{k_1[L_0]}{2} \quad (46)$$

$$\frac{1}{\tau_{BA}} = \frac{k_2[L_0]}{2}; \frac{1}{\tau_{AB}} = \frac{f_B}{f_A}\frac{1}{\tau_{BA}} = \frac{f_B}{f_A}\frac{k_2[L_0]}{2} \quad (47)$$

$$\frac{1}{\tau_{CB}} = k_3; \frac{1}{\tau_{BC}} = \frac{f_C}{f_B}\frac{1}{\tau_{CB}} = \frac{f_C}{f_B}k_3 \quad (48)$$

Hence, when all three exchange processes are active, the reaction scheme corresponds to eq 40, while if exchange between B and C or between one of these and A can be excluded, eq 41 or 42, respectively, will describe the system.

If B ≡ BII, the reaction scheme takes the form:

$$\underset{(C)}{ML_2} + H_2O \underset{k_{-4}}{\overset{k_4}{\rightleftharpoons}} \underset{(BII)}{ML_2(H_2O)} \quad (49)$$

$$\underset{(BII)}{ML_2(H_2O)} + \underset{(A)}{L'} \underset{k_{-5}}{\overset{k_5}{\rightleftharpoons}} \underset{(BII)}{MLL'(H_2O)} + \underset{(A)}{L} \quad (50)$$

From these pseudo-first-order reactions it follows that:

$$\frac{1}{\tau_{CB}} = k_4[H_2O]; \frac{1}{\tau_{BC}} = \frac{f_C}{f_B}\frac{1}{\tau_{CB}} = \frac{f_C}{f_B}k_4[H_2O] \quad (51)$$

$$\frac{1}{\tau_{AB}} = \frac{k_5[L_0]}{2}; \frac{1}{\tau_{BA}} = \frac{f_A}{f_B}\frac{1}{\tau_{AB}} = \frac{f_A}{f_B}\frac{k_5[L_0]}{2} \quad (52)$$

This reaction scheme corresponds to eq 42 assuming $1/\tau_{CA} = 1/\tau_{AC} = 0$. If, in addition, exchange takes place between C and A; that is, if reaction 43 is active, the complete three-way exchange model comes into play.

Finally if B ≡ BIII one must in addition to eq 43 consider the following reaction:

$$\underset{(C)}{ML_2} + \underset{(A)}{L} \underset{k_{-6}}{\overset{k_6}{\rightleftharpoons}} \underset{(BIII)}{ML_3} \quad (53)$$

which, besides eq 46, gives the following exchange rates:

$$\frac{1}{\tau_{BA}} = \frac{k_{-6}}{3}; \frac{1}{\tau_{AB}} = \frac{f_B}{f_A}\frac{k_{-6}}{3} \quad (54)$$

$$\frac{1}{\tau_{CB}} = k_6[L_0]; \frac{1}{\tau_{BC}} = \frac{f_C}{f_B}k_6[L_0] = \frac{2k_{-6}}{3} = \frac{2}{\tau_{BA}} \quad (55)$$

Thus, in this case the general three-way exchange model applies with the restriction that $1/\tau_{BC} = 2/\tau_{BA}$.

The ratio between the two paramagnetic species is given by:

$$\frac{f_B}{f_C} = K \exp\left(-\frac{\delta\Delta H}{RT} + \frac{\delta\Delta S}{R}\right) \quad (56)$$

where $\delta\Delta H = (\Delta H_B - \Delta H_C)$ and $\delta\Delta S = (\Delta S_B - \Delta S_C)$; that is, the difference between the enthalpies and the entropies of formation, respectively, for the two species B and C, while K is a constant, the value of which is determined by the stoichiometry of the complexation reactions.

It is important to notice that the quality of the fit to the experimental data, obtained for each of the three models given by eq 40–42, is independent of the specific nature of the set of first-order complexation reactions that are used in the fit, as long as the reaction scheme is in agreement with the specific model. This is due to the fact that any differences in stoichiometry between different schemes corresponding to the same model only affect the concentration constants in the expressions for the exchange rates and the constant K in eq 56. Thus, for example, in the case of the A ⇄ B ⇄ C exchange scheme one has for B ≡ BI that the exchange rates are given by eq 47 and 48, while the same exchange rates for B ≡ BII are expressed by eq 51 and 52. As to the constant K, it is easily verified from the expressions for the stability constants that it is equal to 1 in the first case, while in the second case it is given by $[H_2O]$. Therefore, only the values obtained for the activation entropies, $\Delta S^{\ddagger}_{ji}$, and for $\delta\Delta S$ will reflect differences between reaction schemes corresponding to the same model. This implies, on the other hand, that an evaluation of the reasonableness of the values obtained by the fit for these parameters can be helpful in selecting the correct reaction scheme, as will be demonstrated below.

D. Determination of the Complexation Reactions. Based on the considerations made in the two preceding sections each one of the three models expressed by eq 40–42 was tested against the experimental data by least-squares fit of the generalized equations for $1/T_{1P}$, $1/T_{2P}$, and $\Delta\omega_P$ derived in section II, with the proper restrictions corresponding to the individual models. In all cases the models were fitted to the three types of data for all six carbons simultaneously. Due to the large stability constant for the $Ni(His)_2$ complexes,[36-40] and because of the considerable surplus of histidine relative to nickel, the amount of Ni^{2+} ions unbound to histidine was assumed to be negligible, so that eq 27 holds. Furthermore, some of the parameters were found to be strongly correlated, showing that the experimental data do not contain information about all the involved parameters, and certain of these were therefore kept fixed at reasonable values. Thus, it was impossible to determine both τ_R^0 and E_R in eq 33 and E_R was given the value 5.9 kcal/mol found for the $Mn(His)_2$ complex[2] under identical experimental conditions, i.e., same pH as well as histidine concentration. Likewise, the three parameters τ_v^0, E_v, and Δ that determine the electron relaxation times are too correlated to be determined independently, and τ_v^0 and E_v were therefore kept equal to the values accepted for these parameters by the $Mn(His)_2$ complex,[2] that is, 8.4×10^{-15} s and 3.9 kcal/mol, respectively. Finally, since only relative distances can be determined from the data, two Ni^{2+}-carbon distances, one in each of the two complexes, were kept at fixed values (vide infra).

With these assumptions the models with only two exchange processes, given by eq 41 and 42, both gave exceptionally good fits, whereas a similar result with the general three-way exchange model in eq 40 was obtained only if $\Delta S^{\ddagger}$ and $\Delta H^{\ddagger}$ for one of the exchange processes were kept fixed at values that correspond to a negligible exchange rate. Also a three-way exchange model in which the restriction $1/\tau_{BC} = 2/\tau_{BA}$, implicitly connected with the formation of the BIII complex according to eq 53–55, disagrees with the data. It must therefore be concluded that only reaction schemes with two exchange processes are compatible with the experimental data.

A general feature shown by all successful fits is an uneven ratio between bidentate and tridentate ligand histidine. Thus, at 298 K this ratio, as calculated from eq 56, is 0.06 when eq 41 is applied and 0.08 when eq 42 is used. Likewise, the distances and coupling constants corresponding to the same histidine carbon, but obtained from different fits agree in all cases within the 1σ uncertainties. Furthermore, as will be discussed in detail below, these parameters for the abundant species correspond closely to the expected C complex, while in the case of the rare complex they are in close agreement with a complex in which a carboxylate group is unbound, as is the case in all B complexes.

In order to proceed and select the proper B species as well as determine the correct complexation reactions one must evaluate the reasonableness of the $\delta\Delta S$ and $\delta\Delta H$ values obtained from the individual multiple regression analysis. These values corresponding to the possible two-exchange-processes reaction schemes described in the preceding section are given

Table II. Apparent Differences in Formation Entropies, $\delta\Delta H$, and Formation Entropies, $\delta\Delta S$, Including 1σ Confidence Limits between the C Complex and the Different B Complexes

	Case	B	K^a	$\delta\Delta H$, kcal mol^{-1}	$\delta\Delta S$, cal mol^{-1} deg^{-1}
Model 1	1	BI	[L]/[L] = 1	4.4 ± 0.3	9.1 ± 1.2
B ⇄ A ⇄ C	2	BII	[H_2O] = 48	4.4 ± 0.3	1.4 ± 1.2
Model 2	3	BI	[L]/[L] = 1	2.5 ± 0.4	3.4 ± 1.3
A ⇄ B ⇄ C	4	BII	[H_2O] = 48	2.5 ± 0.4	−4.3 ± 1.3
	5	BIII	[L] = 1.9	2.5 ± 0.4	2.2 ± 1.3

[a] The constant in eq 56.

in Table II. Notice that a model 1 reaction which involves complex BIII is identical with the above mentioned three-way exchange scheme where $1/\tau_{BC} = 2/\tau_{BA}$ and can therefore be excluded. Also case 2 and 3 in Table II seem rather unlikely, case 2 because it excludes a direct interchange of the labile H_2O molecule in complex BII and the labile COO^- group, and case 3 because it assumes that only ligands in either the tetrahedral or octahedral species, but not both, can exchange with free histidine. However, for the sake of completeness, they have been included.

Before this evaluation can be carried out it is necessary to elucidate what values one should expect for $\delta\Delta H$ and $\delta\Delta S$ in each case. From thermochemical studies of the reactions of transition metal ions with histidine and other amino acids[39,40,50] it has been concluded that the negative values of the enthalpy of formation, ΔH, for the amino acid complexes can be attributed primarily to the formation of covalent bonds between the amino groups and the metal ion. Similarly it has been inferred that the entropy of formation, ΔS, which is positive, is mainly caused by the electrostatic interaction between the carboxylate group of the amino acids and the metal ion because of the resulting decrease of the number of "free" charged ions in the solution.[50] Thus it has been found[39] that ΔH is of the order of −4 kcal mol^{-1} per amino group when a nickel(II)-amino acid complex is formed, while the magnitude of the positive ΔS value depends more upon the individual nature of the amino acid. In agreement with these results the value of ΔH for the complexation of nickel(II) with histidine has been found to be[39,40,51] −16.6, −13.6, and −16.5 kcal mol^{-1}, while the corresponding values for ΔS are 14.9, 28.0, and 15.5 cal mol^{-1} deg^{-1}, respectively.

From these results it is immediately apparent that one should expect a negative value for $\delta\Delta S$ in all cases in Table II, since all three B complexes differ from the C complex in that they have one or more nonchelating carboxylate groups. Furthermore, in the case of complex BI and BII, $\delta\Delta H$ should have a small and positive value, the magnitude of which depends on the covalent nature of the COO^--Ni^{2+} bond, while $\delta\Delta H$ should assume a negative value of the order of −8 kcal mol^{-1} when B is equal to BIII, primarily due to the formation of two covalent bonds between nickel and two amino groups.

As it appears from Table II the values of $\delta\Delta H$ and $\delta\Delta S$ in case 4 are both in close agreement with the expected values, while in the rest of the cases they disagree with what should be expected, especially for $\delta\Delta S$. Thus the value of −4.3 ± 1.3 cal mol^{-1} deg^{-1} obtained for $\delta\Delta S$ in case 4 corresponds to the disengagement of one carboxylate group from the Ni^{2+} ion and should be compared with the average value of −7.5 cal mol^{-1} deg^{-1} per histidine molecule for ΔS obtained by Stack and Skinner[39] under experimental conditions similar to those used in the present study, i.e., [His] ≫ [Ni^{2+}]. Considering the large uncertainty of the value obtained here as well as the fact that ΔS is larger for the first chelating histidine molecule than for the second,[50] the agreement is good. The relatively large value obtained for $\delta\Delta H$, corresponding to a ΔH for the COO^--Ni^{2+} bond of −2.5 ± 0.4 kcal mol^{-1} indicates a relatively high degree of covalency for this bond. Besides the disagreement between the obtained and expected values for $\delta\Delta S$ and $\delta\Delta H$ that holds for the rest of the cases, it should be noted that the models in which the tetrahedral complex BI is involved could be fitted in spite of the fact that the same electron relaxation was assumed for complex BI and C, while one would expect different values for this relaxation time in the two complexes due to their different symmetry. In addition, when extending model 1 to imply different electron relaxation times for the two complexes, the values of these for the two complexes agree within the 1σ uncertainty. Therefore, the data do not give any indication of the presence of a tetrahedral complex; neither are they compatible with any of the possible exchange processes in which BI is one of the paramagnetic sites. This conclusion is supported by the value of the effective magnetic moment given in section IVA. Finally case 5 gives $\tau_{BC}^{-1} < 0.1\tau_{BA}^{-1}$ in the entire experimental temperature range. This is in total conflict with the expected relation $\tau_{BC}^{-1} = 2\tau_{BA}^{-1}$ expressed by eq 55.

From the evaluation of the reasonableness of the data in Table II and other parameters obtained from the multiple regression analysis, it must therefore be concluded that eq 42 most likely represents the exchange scheme for the Ni^{2+}-histidine interaction under the conditions that apply in the present study, and that the two complexes can be identified as complex C and BII of Figure 8. Thus eq 49 and 50 constitute the complexation reactions. These equations correspond closely to the suggested mechanism[6] for the nickel(II)-amino acid complexation, according to which the formation starts with an attack from an amino nitrogen, while the dissociation begins with a detachment of the carboxylate group followed by a cleavage of the Ni-N bonds. The parameters presented below as well as the curves in Figures 5-7 are obtained from a least-squares fit of this model to the experimental data. Finally, due to the relatively high pH (10.4) OH^- could, to a small extent, compete with H_2O as a ligand.[52] This possibility has not been taken into account in the present study.

E. The Dominant Mechanisms of Relaxation. The values of the parameters determining the exchange rates, molecular reorientation, and electron relaxation are given in Table III. Both $\Delta H^{\ddagger}$ values are within the range of 9-13 kcal mol^{-1} normally observed for nickel(II) complexes.[3-9] In particular, the activation parameters for the exchange rates should be

Table III. Parameters Calculated from Experimental Relaxation and Contact Shift Data with 1σ Confidence Limits

$\Delta H^{\ddagger}_{BA}$, kcal mol^{-1}	11.8 ± 0.7	τ_R^0, s	(2.3 ± 0.3) × 10^{-14}
$\Delta S^{\ddagger}_{BA}$, cal mol^{-1} deg^{-1}	−1.4 ± 2.2	E_R, kcal mol^{-1}	5.9[a]
τ_{BA} (298 K), s	(1.4 ± 0.2) × 10^{-4}	τ_R (298 K), s	(4.8 ± 0.7) × 10^{-10}
τ_{BC} (298 K), s	(4.0 ± 0.15) × 10^{-4}	τ_v^0, s	8.4 × 10^{-15}[a]
τ_B (298 K), s	(1.0 ± 0.15) × 10^{-4}	E_v, kcal mol^{-1}	3.9[a]
$\Delta H^{\ddagger}_{CB}$, kcal mol^{-1}	13.6 ± 0.2	Δ, cm^{-1}	1.05 ± 0.04
$\Delta S^{\ddagger}_{CB}$, cal mol^{-1} deg^{-1}	−2.4 ± 0.4	T_{1e} (298 K), s	(8.1 ± 0.6) × 10^{-11}
τ_C (298 K) = τ_{CB} (298 K), s	(4.9 ± 0.2) × 10^{-3}	T_{2e} (298 K), s	(1.1 ± 0.1) × 10^{-11}

[a] See text and ref 2.

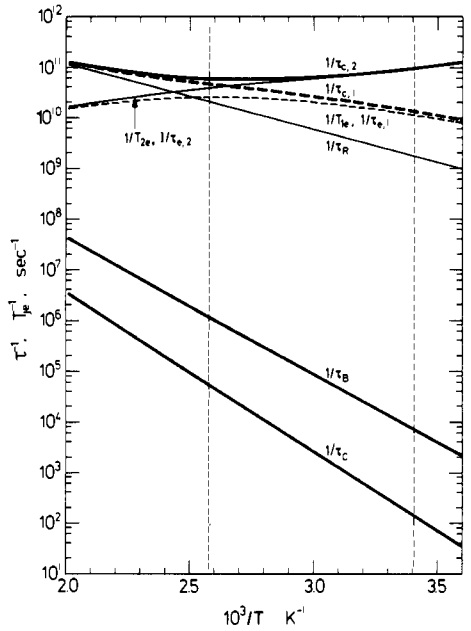

Figure 9. Temperature variation of the electronic spin-lattice relaxation rates, T_{1e}^{-1} and T_{2e}^{-1}, at 23.5 kG, the ligand exchange rates, τ_B^{-1} and τ_C^{-1}, the rotational reorientation rate, τ_R^{-1}, and the sum of these according to eq 30 and 31. The curves were calculated from the relevant parameters in Table III. The dotted lines indicate the experimental temperature region.

compared with $\Delta H^{\ddagger} = 13.2$ kcal mol^{-1} and $\Delta S^{\ddagger} \sim 0$ cal mol^{-1} deg^{-1} found for the nickel(II) complex of oligoglycines.[53] The value obtained for τ_R (298 K) is in close agreement with τ_R (298 K) = $(5.6 \pm 0.2) \times 10^{-10}$ s found for this correlation time in the manganese case,[2] but depends, to some extent, on the value chosen for E_v (vide infra). For both electron relaxation times eq 36 holds, showing that eq 34 and 35 apply in the present case. The obtained T_{1e} and T_{2e} values are both longer than those reported for the aqueous nickel(II) complex[8,10-16] and slightly shorter than values of the order of 2×10^{-10} s at 298 K, reported for other octahedral Ni^{2+} complexes with organic molecules as ligands.[17,18]

The fact that the same τ_v function (τ_v^0 and E_v) as obtained for the $Mn(His)_2$ complex[2] also is consistent with the experimental data in the present study indicates that here, as in the manganese case, the electron relaxation is caused by fluctuations in the symmetry of the complex due to collisions between this and the water molecules,[11,12,54-56] rather than by a static ZFS interaction modulated by the rotational diffusion of the complex,[24,57] in which case $\tau_v \equiv \tau_R$. Because of the strong correlation between E_v, τ_v^0, and Δ, other combinations of E_v and τ_v^0 can be chosen. In fact, equally good fits are obtained for any values of E_v in the range 1-10 kcal mol^{-1} without influencing parameters other than τ_v^0, Δ, and τ_R^0, which vary between 1×10^{-11}-4×10^{-19} s, 1.6-0.8 cm^{-1} and 1.4×10^{-14}-9.5×10^{-15} s, respectively. However, in all cases $\tau_v < 30\tau_R$. Hence, the rotational diffusion of the complex is not providing the modulation mechanism for the electron relaxation. The collision mechanism implies that the ZFS parameter in eq 34 and 35, like its time modulation, results from the impact of the solvent molecules. This transient ZFS parameter should be distinguished from the static ZFS parameter observed for the same complex in the crystal phase, although a static ZFS undoubtedly still is present in the liquid-phase complex. However, since a static ZFS parameter of the order of 1 cm^{-1} is expected to cause some deviation from eq 28-29,[58,59] due to $\omega_{ZFS} \sim \omega_S$, the excellent fit obtained for these equations in the present study indicates that a possible static ZFS interaction is smaller than the obtained value for the transient ZFS interaction. A similar indication of a relatively small static ZFS interaction for a nickel(II) complex in solution is given by Neely and Connick in their study of the nickel hexaquo complex. Thus these authors could account fully for the relaxation of the protons in this complex on the basis of the Solomon-Bloembergen equations and eq 34 and 35, despite the fact that Lindner has shown[59] that considerable deviations from these equations should be expected if a ZFS parameter of 2-2.5 cm^{-1}, as found for $[Ni(H_2O)_6]^{2+}$ in the crystal phase,[35] also was present in the complex in aqueous solution.

Table IV. Electron-Carbon-13 Hyperfine Coupling Constants with 1σ Confidence Limits

	Complex BII	Complex C
(A/h)[C(1)], Hz	$(-1.5 \pm 0.3) \times 10^5$	$(4.31 \pm 0.15) \times 10^5$
(A/h)[C(2)], Hz	$(-3.6 \times 0.6) \times 10^5$	$(-13.90 \pm 0.60) \times 10^5$
(A/h)[C(3)], Hz	$(7.6 \pm 1.0) \times 10^5$	$(3.85 \pm 0.12) \times 10^5$
(A/h)[C(4)], Hz	$(12.5 \pm 1.8) \times 10^5$	$(6.55 \pm 0.24) \times 10^5$
(A/h)[C(5)], Hz	$(12.2 \pm 1.6) \times 10^5$	$(13.03 \pm 0.53) \times 10^5$
(A/h)[C(6)], Hz	$(5.4 \pm 0.7) \times 10^5$	$(15.1 \pm 0.72) \times 10^5$

The relative importance of the pertinent correlation times is shown in Figure 9. As it appears from this figure τ_R^{-1}, T_{1c}^{-1}, and T_{2e}^{-1} differ from each other by only two orders of magnitude or less within the experimental temperature range, while τ_B^{-1} and τ_C^{-1} are negligible compared with these. According to eq 28-31 the relaxation of the carbon nuclei in the metal-bound ligands are therefore entirely determined by the first three correlation times which, on the other hand, all contribute significantly to $\tau_{c,1}$ or $\tau_{c,2}$. This, of course, makes an unraveling of the relaxation pattern less straightforward than in the manganese case, and necessitate a rigorous treatment of the data as in the present study.

The electron-^{13}C hyperfine coupling constants obtained from the multiple regression analysis are given in Table IV. Those found for the aliphatic carbons C(2) and C(3) are in close agreement with the ^{13}C shifts observed by Strouse and Matwiyoff[60] for aqueous solutions of simple aliphatic amino acids (3.0 M) and $NiCl_2$ (1.0 M) at 306 K, both with respect to sign and magnitude. Thus these shifts correspond to coupling constants in the range from -10.7×10^5 to -13.2×10^5 Hz for α carbons and 4.5×10^5 to 6.64×10^5 Hz for the β carbons, when calculating the coupling constants from the shifts[60] by means of eq 38. The upfield shift observed in the present study for C(1) in the lower part of the experimental temperature region is also in qualitative agreement with the results of these authors, even though the magnitude of the shift obtained by them corresponds to a coupling constant between -4.2×10^5 and -5.0×10^5 Hz, and is therefore somewhat larger than what is found for C(1) in the bidentate histidine molecule of the BII complex in the present study. The difference in sign and numerical value between the C(1) coupling constants in complex BII and in complex C is consistent with a disengagement of one of the carboxylate groups from the Ni^{2+} ion in complex BII and is therefore in agreement with the found complexation reaction scheme. The relatively large coupling constant for C(1) in complex C provides evidence for a partly covalent nature of the Ni-O bond in accordance with the relatively large value observed for $\delta\Delta H$. The magnitudes of the coupling constants for the imidazole carbons are close to or within the range of 3.2×10^5-8.6×10^5 Hz found for the carbons in the anilinenickel(II) acetylacetonate complex,[18] but they are all positive in contrast with what is observed for ^{13}C in other aromatic Ni(II) complexes.[18,61,62]

From the correlation times and coupling constants and the distances given below, the T_{1j}^{-1} and T_{2j}^{-1} relaxation rates (j = B, C) and their dipolar and scalar components can now

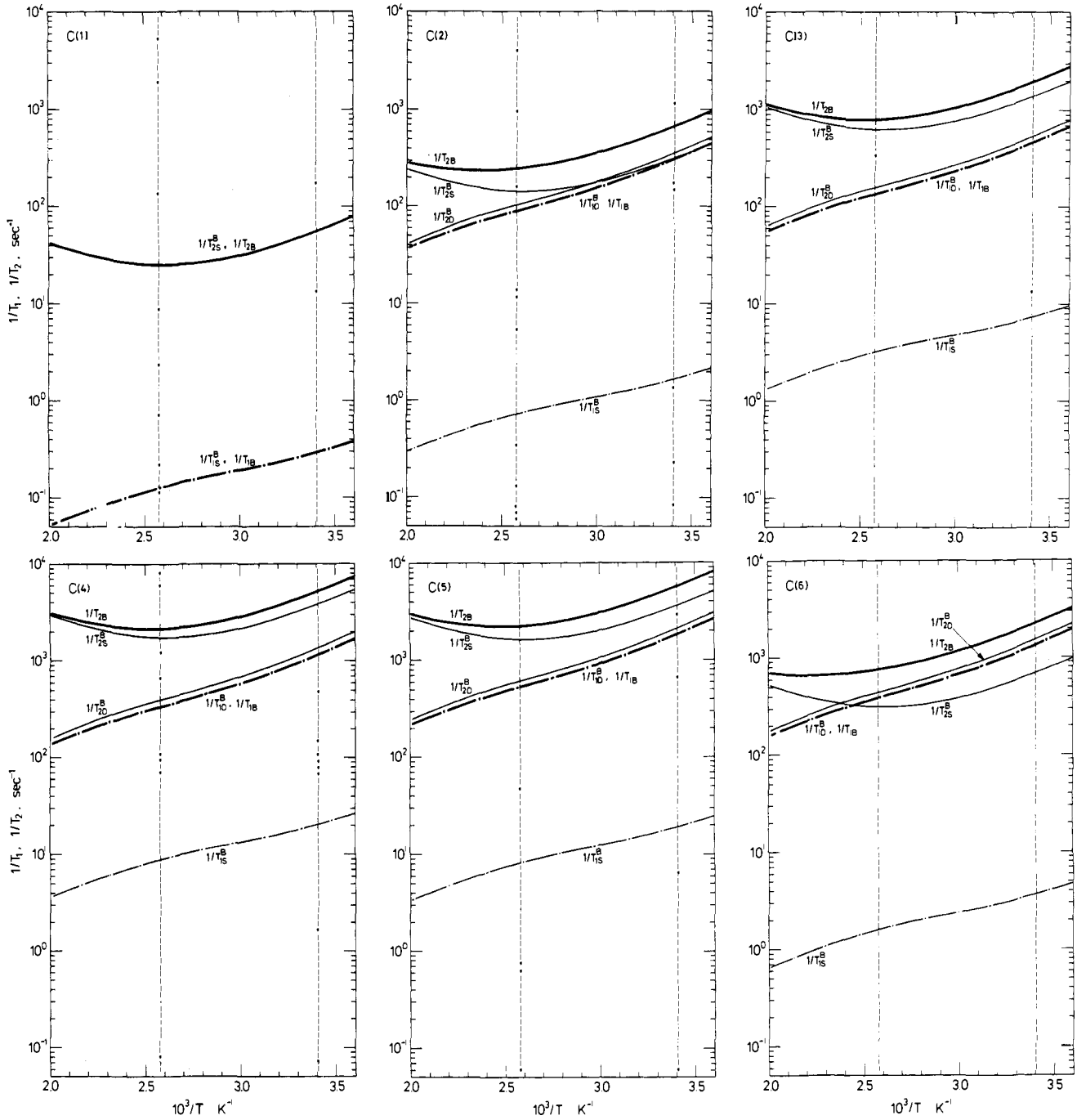

Figure 10. Temperature variation of the spin-lattice and spin-spin relaxation rates and their dipolar and scalar components, at 23.5 kG, for the six individual carbons of histidine, when bound as the bidentate ligand in complex BII (Figure 8). The curves were computed using the relevant parameters in Tables III-V. The dotted lines indicate the experimental temperature region.

be calculated for each one of the six ligand carbons in the two paramagnetic sites. The results are shown in Figures 10 and 11. A general feature of the T_{1j}^{-1} relaxation rates is a negligible scalar contribution. This holds for all carbons in both complexes except C(1) in complex BII, where T_{1B}^{-1} is totally dominated by the scalar term. The T_{2j}^{-1} relaxation rates, on the other hand, are all influenced by both the dipolar and the scalar terms in the experimental temperature region, ranging from dipolar dominance for C(6) in complex BII and for C(1) and C(3) in complex C over almost equal contribution for C(2) in BII and C(4) in C, to a major scalar term in the rest of the cases. The obvious conclusion that can be drawn from these results is that even when the experimental relaxation rates have been corrected for the ligand exchange contribution, a determination of the dipolar and scalar contribution to T_{1j}^{-1} and, especially, T_{2j}^{-1} for the metal-bound ligand carbons, and thereby a determination of distances and coupling constants, is by no means as simple as in the Mn^{2+} case, but requires an extensive treatment of relaxation and shift data.

F. The Structure of the Complexes. As shown above the experimental data are consistent with a complexation reaction scheme that involves the two complexes BII and C. Moreover, the sign and relative magnitudes of the C(1)-electron hyperfine coupling constant support a difference between the two complexes that consist in a nonchelating carboxylate group for the rare species. The obtained Ni^{2+}-carbon distances, however, give more direct information about the structures of the two complexes. These distances are shown in Table V together with the corresponding distances for the bis(histidino)nickel(II) complex taken from the crystal structure.[48] Since only relative

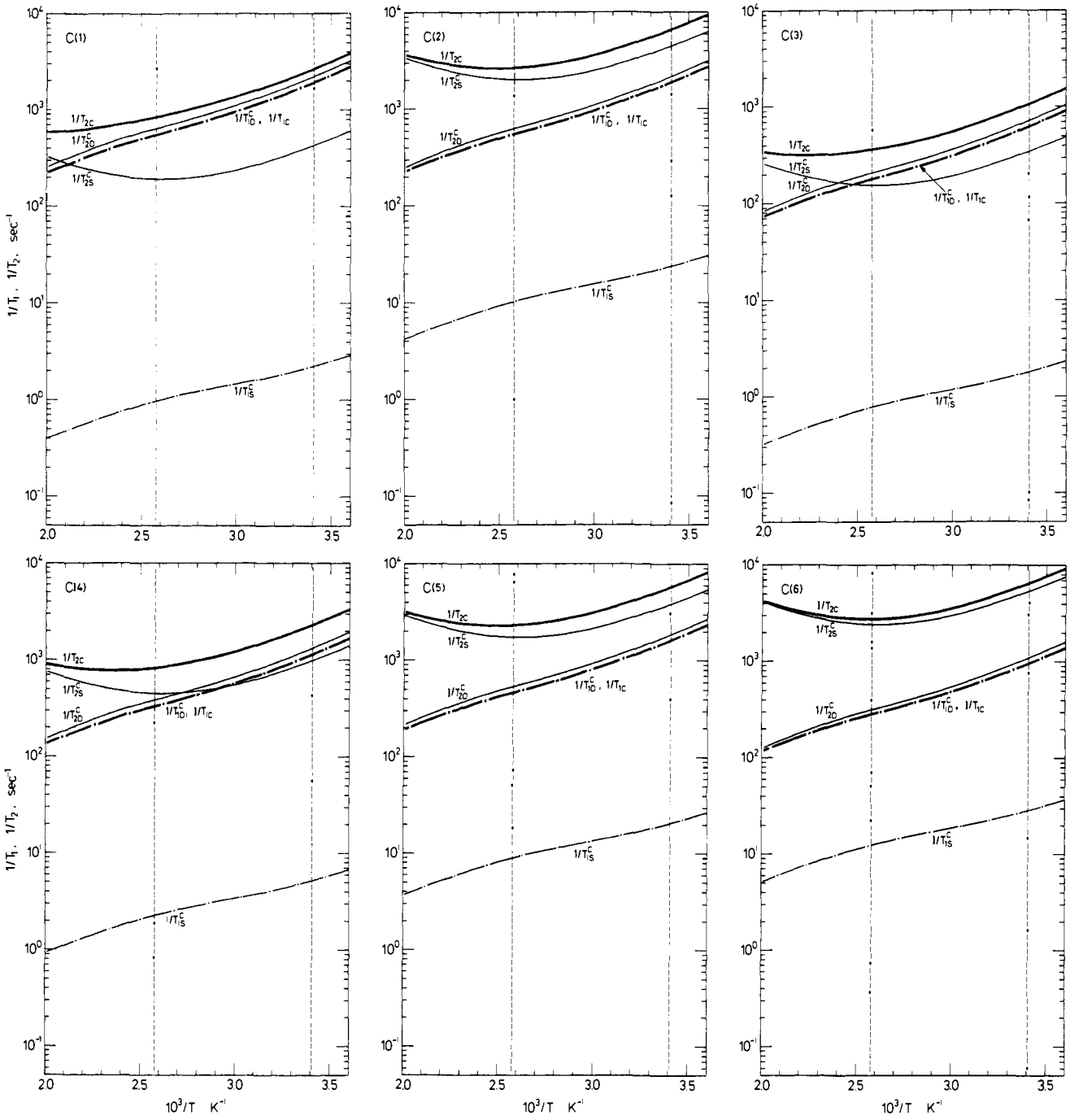

Figure 11. Temperature variation of the spin-lattice and spin-spin relaxation rates and their dipolar and scalar components, at 23.5 kG, for the six individual carbons of histidine when bound in complex C (Figure 8). The curves were computed using the relevant parameters in Tables III-V. The dotted lines indicate the experimental temperature region.

distances can be obtained, two of these are fixed; that is, $r(3)$ in complex C is given the crystal structure value, while in complex B $r(4)$ is kept equal to the value obtained for this parameter in complex C, assuming that the orientation of the imidazole ring relative to the Ni^{2+} ion in the two complexes is the same. As it appears from Table V the values of $r(1)$-$r(5)$ obtained for the abundant species C are in excellent agreement with the crystal phase structure, while $r(6)$ is considerably smaller than the crystal value. A similar pattern was observed in the manganese case.[2] It was there suggested that the enhanced dipolar relaxation of C(6) either was caused by the delocalized electrons not considered in the point dipole approximation used in the Solomon-Bloembergen equations (eq 28-29), or was due to second sphere association of histidine molecules to the metal-bound ligands similar to the hydrogen bonding between histidine molecules, observed in the crystal phase.[48] The same possible explanations might be valid for the disproportionately short distance for C(6) in the present C complex. As for the last mentioned possibility one should expect a substantially higher exchange rate for the hydrogen-bonded histidines than for the metal-bound ones, which again should give rise to appreciable contributions to the experimental data in the lower part of the experimental temperature region. However, the data are inconsistent with such an exchange because of the magnitudes of T_{1P}^{-1}, T_{2P}^{-1}, and $\Delta\omega_P$ in this temperature region, and the possibility is therefore unlikely. The relaxation effect caused by the delocalized electrons can be estimated as[18] $b/(2\rho_i^{\pi})^2$, where ρ_i^{π} is the π spin density on carbon i, while b is the ^{13}C-electron dipolar coupling constant for $\rho^{\pi} = 1$, and is estimated[63] to 4.1×10^8

Table V. Ni^{2+}-C Distances in the Two Observed Histidinonickel(II) Complexes, and the Corresponding Ni^{2+}-C Distances in the Bis(histidino)nickel(II) Complex[48] Obtained by X-Ray Analysis[a]

	Complex B	Complex C	Crystal-phase complex[b]
r(1), Å	c	2.89 ± 0.03	2.83
r(2), Å	3.93 ± 0.24	2.90 ± 0.03	2.84
r(3), Å	3.66 ± 0.25	3.49[d]	3.49
r(4), Å	3.15[d]	3.15 ± 0.04	3.13
r(5), Å	2.92 ± 0.08	2.97 ± 0.04	3.06
r(6), Å	3.09 ± 0.08	3.25 ± 0.04	4.27

[a] The indicated errors are the 1σ confidence limits. [b] The estimated standard deviations of the bond length in the Ni^{2+} complex are reported to be 0.01-0.02 Å.[48] [c] Not obtainable from the experimental data, see text. [d] Assumed values, see text.

s^{-1}. ρ_i^{π} can be calculated from the McConnell equation[28,64]

$$A_H = \frac{Q\rho_i^{\pi}}{2S} \quad (57)$$

A_H being the electron-proton hyperfine coupling constant for the proton attached to the carbon in question, while $Q = -22.5$ G. A rough estimate of A_H can be obtained from the downfield shift of 40-50 ppm reported[65] for the imidazole protons in the $Ni(His)_2$ complex. By using eq 38 and 57 one obtains $\rho_i^{\pi} = 0.02$ for $S = 1$, resulting in a ^{13}C-electron dipolar interaction for the carbon-centered electron density of the same order of magnitude as for the metal-centered electrons given by the dipole-dipole coupling constant, $(g\beta\gamma_C)^2/r^6$, in eq 28. Therefore, despite the approximations involved in the calculations, in particular the neglect of a possible Fermi contact contribution[61] to the observed proton shifts, it seems likely that the enhanced relaxation of C(6) in complex C is caused by the ligand-centered non-s spin density. Other authors[66,67] have arrived at the same conclusion in the case of Cu^{2+} and Mn^{2+} complexes of imidazole. An evaluation of ρ^{π} on the basis of the electron-carbon hyperfine coupling constants obtained in the present work is far more complicated[68] than using A_H and eq 57, not only because of the complex relation[69] between these coupling constants and ρ^{π}, but also because the ^{13}C shift could, at least in part, be due to Fermi contact interaction.[61]

In the BII complex the value obtained for r(5) agrees with that obtained for the same parameter in complex C, supporting the assumption of equal orientation of the ring relative to Ni^{2+} in the two complexes. Despite a small value for A[C(1)] in complex BII, the dipolar contribution to T_{1B}^{-1} is found to be negligible compared with the scalar term, showing that r(1) is long and cannot be determined from the data. This is consistent with the demonstrated reaction scheme as well as with the sign and magnitudes of the A[C(1)] coupling constants in the two complexes in that it agrees with a carboxylate group detached from the Ni^{2+} ion in the rate species. Compared with the corresponding distances in complex C and the crystal phase structure, r(3) is within the 1σ limits, while r(2) is considerably larger. Even though a nonchelating carboxylate group will give rise to a longer r(2) than in complex C, it still seems too large a value considering that the maximum value possible is about 3.6 Å, corresponding to a Ni-N-C(2) angle of 180°. However, a lengthening of the Ni-N bond due to a beginning breakage could be of importance, or the obtained value could correspond to an average of two structures, BII and one in which the α-amino group also has been detached from the Ni^{2+} ion. The small value of A[C(2)] in complex B compared to complex C as well as the relatively high value for $\delta\Delta H$ is in agreement with these suggestions. Finally, r(6) is inordinately short as in complex C. Also here this is most likely due to electron delocalization.

V. Conclusion

As revealed by the present study, the interpretation of relaxation and shift data for ^{13}C nuclei in a Ni^{2+} complex in aqueous solution is not only complicated by the competition between different correlation times and between different relaxation mechanisms, but also by the presence of at least two distinguishable complexes. This stresses the caution one must exercise when interpreting such data, especially when only one type of these is available in a narrow temperature range or, even worse, at a single temperature. On the other hand, when a complete unraveling of the relaxation and shift data over a large temperature range is performed, precise information about complexation reactions, complex ratio and structures, relaxation mechanisms, and carbon-13-electron hyperfine coupling constants can be gained.

Acknowledgment. This work was supported in part under Grant RR-574 provided by the Research Resource section of the National Institute of Health. J.J.L. was the recipient of a travel grant from the Danish Scientific Research Council.

Supplementary Material Available: Tables containing the experimental $1/T_1^0$, $1/T_{1,obsd}$, and $1/T_{1P}$ data corresponding to Figures 2 and 5 (Tables VI and VII) as well as the line width data corresponding to Figure 6 (Table VIII) and the chemical shift and contact shift data corresponding to Figure 7 (Table IX) (24 pages). Ordering information is given on any current masthead page.

References and Notes

(1) (a) University of Copenhagen; (b) University of Utah.
(2) J. J. Led and D. M. Grant, *J. Am. Chem. Soc.*, **97**, 6962 (1975), and references cited therein.
(3) M. Eigen and R. G. Wilkins, *Adv. Chem. Ser.*, **No. 49**, 55 (1965), and references cited therein.
(4) T. R. Stengle and C. H. Langford, *Coord. Chem. Rev.*, **2**, 349 (1967), and references cited therein.
(5) K. Kustin and J. Swinehart, *Prog. Inorg. Chem.*, **13**, 107 (1970), and references cited therein.
(6) R. G. Wilkins, *Acc. Chem. Res.*, **3**, 408 (1970); *Pure Appl. Chem.*, **33**, 583 (1973).
(7) Z. Luz and S. Meiboom, *J. Chem. Phys.*, **40**, 2686 (1964).
(8) T. J. Swift and R. E. Connick, *J. Chem. Phys.*, **37**, 307 (1962); **41**, 2553 (1964).
(9) Z. Luz and S. Meiboom, *J. Chem. Phys.*, **40**, 1066 (1964).
(10) L. O. Morgan and A. W. Nolle, *J. Chem. Phys.*, **31**, 365 (1959).
(11) N. Bloembergen and L. O. Morgan, *J. Chem. Phys.*, **34**, 842 (1961).
(12) W. B. Lewis and L. O. Morgan, *Transition Met. Chem.*, **4**, 33 (1968).
(13) D. Forster, *Inorg. Chim. Acta*, **2**, 116 (1968).
(14) R. E. Connick and D. Fiat, *J. Chem. Phys.*, **44**, 4103 (1966).
(15) A. M. Chmelnick and D. Fiat, *J. Chem. Phys.*, **49**, 2101 (1968); *J. Am. Chem. Soc.*, **93**, 2875 (1971).
(16) J. W. Neely and R. E. Connick, *J. Am. Chem. Soc.*, **94**, 3419 (1972).
(17) I. D. Campbell, I. P. Carver, R. A. Dwek, A. F. Nummelin, and R. E. Richards, *Mol. Phys.*, **20**, 913 (1971).
(18) C. Chachaty, A. Forchini, J. Virlet, and J. C. Ronfard-Haret, *Chem. Phys. Lett.*, **29**, 436 (1974); *Can. J. Chem.*, **53**, 648 (1975); *Mol. Phys.*, **31**, 325 (1976).
(19) Y.-F. Lam, G. P. P. Kuntz, and G. Kotowycz, *J. Am. Chem. Soc.*, **96**, 1834 (1974).
(20) H. M. McConnell, *J. Chem. Phys.*, **28**, 430 (1958).
(21) I. Solomon, *Phys. Rev.*, **99**, 559 (1955).
(22) N. Bloembergen, *J. Chem. Phys.*, **27**, 572 (1957).
(23) J. Reuben, G. H. Reed, and M. Cohn, *J. Chem. Phys.*, **52**, 1617 (1970).
(24) A. Carrington and G. R. Luckhurst, *Mol. Phys.*, **8**, 125 (1964).
(25) A. D. McLachlan, *Proc. R. Soc. London, Ser. A*, **280**, 271 (1964).
(26) A. G. Redfield, *IBM J. Res. Dev.*, 1, 19 (1957); *Adv. Magn. Reson.*, 1, 1 (1965).
(27) N. Bloembergen, *J. Chem. Phys.*, **27**, 595 (1957).
(28) H. M. McConnell and D. B. Chesnut, *J. Chem. Phys.*, **28**, 107 (1958).
(29) R. Freeman and H. D. W. Hill, *J. Chem. Phys.*, **51**, 3140 (1969).
(30) G. C. Levy and I. R. Peat, *J. Magn. Reson.*, **18**, 500 (1975).
(31) R. R. Ernst, *Adv. Magn. Reson.*, **2**, 1 (1966).
(32) D. F. Evans, *J. Chem. Soc.*, 2003 (1959).
(33) J. L. Deutsch and S. M. Poling, *J. Chem. Educ.*, **46**, 167 (1969).
(34) T. Nortia, *Suom. Kemistil. B*, **33**, 161 (1960).
(35) K. H. Hellwege and A. M. Hellwege, Ed., "Magnetic Properties of Transition Metal Compounds", Springer-Verlag, New York, N.Y., 1966; B. R. McGarvey, *Transition Met. Chem.*, **3**, 89 (1966).
(36) A. Albert, *Biochem. J.*, **50**, 690 (1952).
(37) R. H. Carlson and T. L. Brown, *Inorg. Chem.*, **5**, 268 (1966).
(38) D. D. Perrin and V. S. Sharma, *J. Chem. Soc. A*, 724 (1967).
(39) W. F. Stack and H. A. Skinner, *Trans. Faraday Soc.*, **63**, 1136 (1967).
(40) E. V. Raju and H. B. Mathur, *J. Inorg. Nucl. Chem.*, **31**, 425 (1969).
(41) Reference 2, Figure 5.
(42) H. M. McConnell and R. E. Robertson, *J. Chem. Phys.*, **29**, 1361 (1958).
(43) J. P. Jesson, *J. Chem. Phys.*, **47**, 579, 582 (1967).

(44) B. R. McGarvey, *J. Chem. Phys.*, **53**, 86 (1970).
(45) B. R. McGarvey, *J. Am. Chem. Soc.*, **94**, 1103 (1972).
(46) R. J. Kurland and B. R. McGarvey, *J. Magn. Reson.*, **2**, 286 (1970).
(47) G. N. LaMar, G. R. Eaton, R. H. Holm, and F. A. Walker, *J. Am. Chem. Soc.*, **95**, 63 (1973).
(48) K. A. Fraser and M. M. Harding, *J. Chem. Soc. A*, 415 (1967).
(49) C. C. McDonald and W. D. Phillips, *J. Am. Chem. Soc.*, **85**, 3736 (1963).
(50) V. S. Sharma and H. B. Mathur, *Indian J. Chem.*, **3**, 475 (1965).
(51) D. S. Barnes and L. D. Pettit, *J. Inorg. Nucl. Chem.*, **33**, 2177 (1971).
(52) J. C. Cassatt, W. A. Johnson, L. M. Smith, and R. G. Wilkins, *J. Am. Chem. Soc.*, **94**, 8399 (1972).
(53) G. Davies, K. Kustin, and R. F. Pasternack, *Inorg. Chem.*, **8**, 1535 (1969).
(54) M. Rubinstein, A. Baram, and Z. Luz, *Mol. Phys.*, **20**, 67 (1971).
(55) H. Levanon, G. Stein, and Z. Luz, *J. Chem. Phys.*, **53**, 876 (1970).
(56) H. Levanon, S. Charbinsky, and Z. Luz, *J. Chem. Phys.*, **53**, 3056 (1970).
(57) B. R. McGarvey, *J. Phys. Chem.*, **61**, 1232 (1957).
(58) R. A. Dwek, "Nuclear Magnetic Resonance in Biochemistry", Clarendon Press, Oxford, 1973, p 185.
(59) U. Lindner, *Ann. Phys.*, **16**, 319 (1965).
(60) C. E. Strouse and N. A. Matwiyoff, *J. Chem. Soc. D*, 439 (1970).
(61) D. Doddrell and J. D. Roberts, *J. Am. Chem. Soc.*, **92**, 4484, 5255, 6839 (1970).
(62) I. Morishima, K. Okada, K. Goto, and T. Yonezawa, *J. Chem. Soc. D*, 1535 (1970); *J. Am. Chem. Soc.*, **92**, 6651 (1970); **94**, 1425 (1972).
(63) M. Barfield, *J. Chem. Phys.*, **53**, 3836 (1970).
(64) H. M. McConnell, *J. Chem. Phys.*, **24**, 764 (1956); *Proc. Natl. Acad. Sci. U.S.A.*, **43**, 721 (1957).
(65) R. S. Milner and L. Pratt, *Discuss. Faraday Soc.*, **34**, 88 (1962).
(66) W. G. Espersen, W. C. Hutton, S. T. Chow, and R. B. Martin, *J. Am. Chem. Soc.*, **96**, 8111 (1974); **98**, 40 (1976); *J. Phys. Chem.*, **80**, 161 (1976).
(67) R. E. Wasylishen and M. R. Graham, *Can. J. Chem.*, **54**, 617 (1976).
(68) G. N. LaMar, "NMR of Paramagnetic Molecules", G. N. LaMar, W. D. W. Horrocks, and R. H. Holm, Ed., Academic Press, New York, N.Y., 1965, p 85.
(69) M. Karplus and G. K. Fraenkel, *J. Chem. Phys.*, **35**, 1312 (1961).

Carbon-13 Fourier Transform Nuclear Magnetic Resonance Study of Gallium Citrate in Aqueous Solution[1]

C. H. Francis Chang, T. Phil Pitner, Robert E. Lenkinski, and Jerry D. Glickson* [2]

Contribution from the Departments of Physics, Chemistry, Biochemistry, and Medicine (Hematology Oncology) and the Comprehensive Cancer Center, University of Alabama in Birmingham, Birmingham, Alabama 35294. *Received August 4, 1976*

Abstract: As a basis for understanding the molecular mechanism of gallium localization in tumor cells, the aqueous chemistry of gallium citrate in D_2O at 31 °C was investigated by ^{13}C FT-NMR spectroscopy (22.63 MHz). Complexes of the form Ga_n-$(citrate)_{2n}$ were detected at neutral or mildly acidic pD_c's when the molar concentration of citrate was equal to or greater than the molar concentration of added gallium. In this complex, chemical exchange of bound citrate with free citrate is slow on the ^{13}C NMR time scale. Line broadening of the citrate resonances as well as decreases in their apparent ^{13}C spin-lattice relaxation times (T_1) indicated formation of gallium citrate polymers in moderately acidic solutions at equal concentrations of gallium and citrate and in neutral solutions when the gallium/citrate concentration ratio was larger than 0.50. The "average diameter" of the polymer, estimated from the line width of the broad citrate CH_2 resonance of gallium/citrate 1 M/1 M, was 50 Å at pD_c 7.40 and 40 Å at pD_c 2.75. The properties of gallium citrate complexes have been compared with those of ferric citrate.

As part of a program to define the molecular mechanism of action of gallium tumor scanning agents,[3] this laboratory has been investigating the biological properties and aqueous chemistry of various gallium salts.[4] The citrate salt is particularly important because gallium radioisotopes are clinically administered as citrate buffered solutions, because the extent of gallium localization in certain model tumor systems depends on the citrate concentration,[4a-e] and because citrate may play a significant role in serum transport of this metal. In a recent study of gallium citrate in D_2O solution by ^1H and ^{71}Ga NMR,[4f] this laboratory demonstrated that the type of complex formed depends on both the pD_c (pH meter reading +0.40) of the solution and on the relative concentration of the metal and ligand. A 1/1 gallium citrate complex (GaCit), gallium citrate polymers, and a low molecular weight gallium citrate complex of undetermined stoichiometry were detected under various experimental conditions. The present ^{13}C FT-NMR study was undertaken to further characterize some of the gallium citrate complexes detected in the previous study.[4f] By this method it was possible to confirm the observations made in the previous study, to determine the stoichiometry of the previously uncharacterized low molecular weight complex, and to estimate the average dimensions of the gallium citrate polymers. Taken together with the previous ^1H and ^{71}Ga NMR study these investigations demonstrate some striking similarities between the aqueous chemistry of citrate complexes of gallium(III) and iron(III).

Experimental Section

Materials. $Ga(NO_3)_3 \cdot 9H_2O$ (Alfa Inorganic, Beverly, Mass.), trisodium citrate monohydrate (Fisher Scientific Co., Fair Lawn, N.J., certified reagent), citric acid monohydrate (Matheson Coleman and Bell, East Rutherford, N.J., A.C.S. reagent), and D_2O (Aldrich Chemical Co., Milwaukee, Wis.) were used as commercially supplied. In D_2O solution the pD_c was adjusted with DCl (Stohler Isotope Chemicals, Azusa, Calif.) and NaOD (Stohler Isotope Chemicals, Azusa, Calif.). Care was taken to remove paramagnetic impurities by soaking all glassware in EDTA solution before use.

NMR Spectra. Natural abundance ^{13}C FT-NMR spectra (4K transforms) were measured at 22.63 MHz with a Bruker HX-90-18 spectrometer system (single coil) equipped with a NIC-1085 data system (Nicolet Instrument Corp., Madison, Wis.). Field-frequency lock was established using the deuterium resonance of D_2O. In some experiments a Bruker B-SV2 pulse amplifier (90° pulse width 8-10 μs) was employed; other experiments were performed with an ENI 3100L broad band amplifier (Electronic Navigation Industries, Rochester, N.Y.; 90° pulse width about 30 μs). In order to ensure equilibration of spins in all FT-NMR and nuclear Overhauser effect (NOE) experiments, the recycling time between scans was at least five times the longest citrate methylene T_1. NOE's were measured by comparing peak intensities obtained with continuous ^1H decoupling and intensities obtained with ^1H decoupling gated on only during data acquisition. T_1 values were determined by means of a $(180°-\tau-90°-t)$ pulse sequence,[5] where τ is a variable delay time and t is at least four times the longest T_1 of the citrate methylene resonances. Unless otherwise specified, all spectra were measured at ambient probe temperature (31 °C) with broad band ^1H decoupling and air cooling.